

N70 32465

NASA CR 110642

TM-70-2034-4

**TECHNICAL
MEMORANDUM**

**THE OPTIMUM PHASE DEMODULATOR FOR
INTERFERING PM SUBCARRIER SIGNALS**

**CASE FILE
COPY**

Bellcomm

BELLCOMM, INC.

955 L'ENFANT PLAZA NORTH, S.W., WASHINGTON, D.C. 20024

COVER SHEET FOR TECHNICAL MEMORANDUM

TITLE- The Optimum Phase Demodulator for
Interfering PM Subcarrier Signals.

TM-70-2034-4

FILING CASE NO(S)- 320

DATE- June 3, 1970

FILING SUBJECT(S)-
(ASSIGNED BY AUTHOR(S))- Demodulators for PM
Signals

AUTHOR(S)- W. D. Wynn

ABSTRACT

In a previous memorandum (TM-69-2034-7) a procedure was discussed for deriving optimum linear phase-locked loop (PLL) FM receivers that demodulate Unified S-Band type signals with minimum mean square errors. However, the subcarrier signals were assumed to be non-overlapping in the subcarrier frequency band, and the optimization was constructive in that the PLL forms for the demodulators were presupposed by experience.

The following report presents the derivation of an optimum demodulator that produces minimum mean square error estimates of interfering subcarrier signals that are phase modulated as a sum on a carrier. These subcarrier signals are interfering in that they overlap in the subcarrier band. The derivation presented here is nonconstructive in that no a priori knowledge of the form the demodulator should have is assumed. The approach taken here is considerably more general than that in the previous memorandum mentioned, and can be applied to find receivers for signals that are more complex than interfering frequency multiplexed FM or PM subcarrier signals.

An example is considered where there are two PM subcarrier signals that overlap in the subcarrier band. One has a broadband video spectrum and the other has a narrow bandpass spectrum centered about a subcarrier frequency. The spectra for these subcarrier signals is chosen to simulate the problem of simultaneously demodulating interfering TV and bandpass voice signals. This problem is encountered in the system used to transmit Apollo color TV from moon to earth.

DISTRIBUTIONCOMPLETE MEMORANDUM TO

CORRESPONDENCE FILES:

OFFICIAL FILE COPY

plus one white copy for each
additional case referenced

TECHNICAL LIBRARY (4)

NASA Headquarters

B. P. Brown/MOR
S. W. Fordyce/MLA
J. K. Holcomb/MAO
T. A. Keegan/MA-2
A. W. Kinny/MOP
J. T. McClanahan/MOR
L. M. Robinson/TS
J. D. Stevenson/MO
W. E. Stoney/MA

MSC

G. D. Arndt/EB2
B. H. Batson/EB2
E. L. Chicoine/EE3
J. A. Frere/FS4
H. C. Kyle/EB
C. K. Land/EB2
J. McKenzie/PD4
R. W. Moorehead/EB2
L. Packham/EE
S. D. Sanborn/FS4
R. S. Sawyer/EE
W. E. Zrubek/EE3

MSFC

T. A. Barr/R-ASTR-IR
H. R. Lowery/R-ASTR-IRC
L. B. Malone/R-ASTR-IRC
J. T. Powell/R-ASTR-I
J. Cox

GSFC

O. M. Covington/800
A. F. Grandinetti/834
T. Roberts/810
J. P. Shaughnessy/834
W. P. Varson/830

TRW, Inc.

R. P. Liccini
R. P. Tow, Jr.

JPL

R. C. Tausworthe

Bellcomm, Inc.

G. M. Anderson
W. J. Benden
A. P. Boysen, Jr.
R. K. Chen
L. A. Ferrara
D. R. Hagner
H. A. Helm
J. J. Hibbert
B. T. Howard
D. B. James
J. E. Johnson
H. Kraus
S. Y. Lee
J. P. Maloy
J. Z. Menard
L. D. Nelson
B. F. O'Brien
J. T. Raleigh
I. I. Rosenblum
I. M. Ross
N. W. Schroeder
L. Schuchman
R. L. Selden
R. V. Sperry
J. W. Timko*
B. P. Tunstall
R. L. Wagner
A. G. Weygand
M. P. Wilson
Department 1024 File

*Abstract Only

SUBJECT: The Optimum Phase Demodulator For
Interfering PM Subcarrier Signals
Case 320

DATE: June 3, 1970

FROM: W. D. Wynn

TM- 70-2034-4

TECHNICAL MEMORANDUM

1.0 INTRODUCTION

A well known method for transmitting N signals $a_i(t)$, $i=1, \dots, N$ using a single carrier $\sqrt{2P} \sin \omega_c t$ is to frequency multiplex the N signals and phase modulate the carrier with the

sum $x = \beta_c \sum_{i=1}^N a_i(t)$. The resulting transmitted waveform is

$s(t) = \sqrt{2P} \sin[\omega_c t + x(t)]$. In frequency multiplexing $a_i(t)$, $i=1, \dots, N$, sufficient subcarrier bandwidth must be allocated if there is to be no interference of the subcarriers. For this restraint on the subcarriers, $S_i(\omega)S_j(\omega) \equiv 0$ for all ω and $i \neq j$ where $i, j=1, 2, \dots, N$.

In a previous memorandum a procedure was discussed for finding an optimum linear demodulator in the minimum-mean-square error sense for demodulating $a_i(t)$, $i=1, \dots, N$, when the spectra $S_i(\omega)$, $i=1, \dots, N$, did not overlap in the subcarrier frequency band (ref.1). With this demodulator, estimates were made of $a_i(t)$ at time t given $s(\tau) + n(\tau)$, $-\infty < \tau \leq t$ where $n(t)$ was white Gaussian noise. For a sufficient input SNR, the demodulator was realized as a phase locked loop and the solution for the components of this loop was performed by considering each subcarrier independently of the other $N-1$ members of $x(t)$.

An example where the subcarrier spectra are orthogonal such that $S_i(\omega) S_j(\omega) \equiv 0$ for $i \neq j$ is the original television system used on the lunar surface. The design provided a 0.5 MHz bandwidth TV subcarrier signal that was transmitted to earth by the Lunar Module's S-Band system. Frequency multiplexed with this TV signal were two subcarriers at 1.024 MHz and 1.25 MHz carrying pulse code modulation telemetry and voice and biomedical telemetry (ref.2).

In some systems the orthogonal property of the subcarrier spectra may not hold. This was the situation when the S-Band television signal was changed from a 0.5 MHz black-and-white to 2.0 MHz color baseband signal. With this change some signal processing after demodulation is required to reduce the interference in the TV signal caused by the voice and telemetry subcarriers around 1 MHz. The amount of interference between the overlaying subcarriers is a function of the positions of the voice and telemetry subcarrier spectra with respect to the color TV spectrum and the phase modulation indices of the subcarriers.

In the present memorandum a demodulator is derived for estimating subcarrier signals $a_i(t)$, $i=1, \dots, N$, given $s(\tau) + n(\tau)$, $-\infty < \tau \leq t$, where the modulation components interfere in the subcarrier band. The noise $n(t)$ is assumed to be white and Gaussian with a two-sided spectral density $N_0/2$ watts/Hz. The demodulator derived is asymptotically optimum with respect to mean square error for large values of the carrier power-to-noise density ratio $2P/N_0$. Expressions are obtained for the performance

of the demodulator above threshold. This performance is measured in terms of the mean square errors in estimating $a_i(t)$, $i=1, \dots, N$, as functions of $2P/N_0$ and the carrier phase modulation index β_c .

2.0 DISCUSSION

2.1 System Assumptions

In this section an optimum demodulator is derived for estimating subcarrier signals $a_i(t)$, $i=1, \dots, N$ from an input signal-plus-noise of the form $s(\tau)+n(\tau) = \sqrt{2P} \sin[\omega_c \tau + x(\tau)]+n(\tau)$

where $x(\tau) = \beta_c \sum_{i=1}^N a_i(\tau)$, and $-\infty < \tau \leq t$. The requirement $-\infty < \tau \leq t$ means the estimator will be realizable in that only past knowledge of $s+n$ is used to estimate $a_i(t)$ and no knowledge of the future of $s+n$ is necessary.

The following assumptions will be made in the derivation of the optimum demodulator.

- (1) The received waveform is $s(\tau)+n(\tau)$, $-\infty < \tau \leq t$, where $s(\tau) = \sqrt{2P} \sin[\omega_c \tau + x(\tau)]$ with P and ω_c constants and $x(t) = \beta_c \sum_{i=1}^N a_i(t)$. The interference is $n(t)$, an additive white Gaussian noise, with zero mean and a two-sided power spectral density equal to $N_0/2$ watts/Hz.
- (2) In $x(t)$, β_c is a positive constant and each $a_i(t)$ is a stationary Gaussian process with

zero mean and an autocorrelation function $R_i(\tau)$. The Gaussian assumption for the $a_i(t)$ is not unrealistic for some communication problems, but there are many cases where its use is questionable. The Gaussian assumption is no more restrictive than assuming knowledge about only the mean and autocorrelation function of a random process. Working only with the mean value and autocorrelation function is often the only useful approach in nonlinear modulation problems. The power spectrum of $a_i(t)$ given by $S_i(\omega) = F[K_i(\tau)]$ has frequency components that are very low compared to ω_c . That is, $x(t)$ has a video spectrum with an upper cut-off frequency that is small compared to ω_c . Usually the signal spectra $S_i(\omega)$ are assumed to be rational. Any signal model with a non-rational spectrum can normally be approximated by a signal that has a rational spectrum (ref.3).

- (3) The interference $n(t)$ and the $a_i(t)$, $i=1, \dots, N$, are mutually independent random processes. Then $K_{a_i n}(t_1, t_2) = 0 = K_{a_i a_j}(t_1, t_2)$ for $1 \leq i, j \leq N$ and $i \neq j$. Of course, the spectra $S_i(\omega)$

may overlap in the subcarrier band even though the $a_i(t)$ are independent processes.

- (4) The criterion for optimization is the minimization for each $i=1, \dots, N$ of the mean-square error (MMSE) $a_{\epsilon_i}(t)$ between the true value $a_i(t)$ and the estimate $\hat{a}_i(t)$ made with the demodulator. In other words the expectations $E[(\hat{a}_i(t) - a_i(t))^2]$, $i=1, \dots, N$, are minimized. This is a point estimation criterion in that the past and present values of $s+n$ are processed to give a MMSE estimate of $a_i(t)$, $i=1, \dots, N$ at the present point in time t .

2.2 Optimum Demodulator For $a_i(t)$

The problem posed here is one of multidimensional waveform estimation at time t where the modulation technique is nonlinear but without memory. If $\underline{a}(t)$ and $\underline{a}_\epsilon(t)$ define the column vectors

$$\underline{a}(t) = \begin{bmatrix} a_1(t) \\ \cdot \\ \cdot \\ \cdot \\ a_N(t) \end{bmatrix} \quad \text{and} \quad \underline{a}_\epsilon(t) = \begin{bmatrix} \hat{a}_1(t) - a_1(t) \\ \cdot \\ \cdot \\ \cdot \\ \hat{a}_N(t) - a_N(t) \end{bmatrix} \quad (1)$$

the received waveform to be demodulated is a scalar function of $\underline{a}(t)$,

$$\begin{aligned} r(t) &= s(t, \underline{a}(t)) + n(t) \\ &= \sqrt{2P} \sin \left[\omega_c t + \beta_c \sum_{i=1}^N a_i(t) \right] + n(t) , \end{aligned} \quad (2)$$

and the mean square error in estimating $\underline{a}(t)$ at time t is

$$\epsilon(t) = E[\underline{a}_\epsilon^T(t) \underline{a}_\epsilon(t)] , \quad (3)$$

where T denotes the transpose of a column vector.

To find the demodulator that minimizes (3), a direct approach could be taken analogous to the approach that leads to the Wiener-Hopf integral equation in linear modulation problems (ref.4, sec.6.1). A direct approach has been used by Snyder (ref.5). Alternately in this memorandum the MMSE demodulator is found indirectly by first obtaining the maximum a posteriori (MAP) interval estimator for $\underline{a}(t)$ on the interval $(-\infty, t]$ (ref.4, chapt.5). This indirect approach is easier to follow than that taken in reference 4. A discussion of MAP interval estimators and the derivation of the estimator for the received waveform (2) are provided in Appendix I. From Appendix I the MAP interval estimates are

$$\hat{a}_i(t') = \frac{2}{N_0} \int_{-\infty}^t K_i(t'-z) \frac{\partial s(z, \hat{\underline{a}}(z))}{\partial \hat{a}_i(z)} [r(z) - s(z, \hat{\underline{a}}(z))] dz \quad (4)$$

for $-\infty < t' \leq t$ and $i=1, \dots, N$. Here $r(z)$ is the received waveform and

$$\frac{\partial s(z, \hat{a}_i(z))}{\partial \hat{a}_i(z)} = \beta_c \sqrt{2P} \cos[\omega_c z + \hat{x}(z)] , \quad i=1, \dots, N . \quad (5)$$

The estimate $\hat{a}_i(t')$, $-\infty < t' \leq t$ is the convolution of a filter impulse response $K_i(t')$, $-\infty < t' \leq t$ and an input signal. Since $K_i(\tau)$ is the autocorrelation function of $a_i(t)$ where $S_i(\omega)$ has frequency components that are very low compared with ω_c ; $\hat{a}_i(t')$, $-\infty < t' \leq t$, is also given by the convolution

$$\hat{a}_i(t') = \frac{2}{N_0} \int_{-\infty}^{+\infty} K_i(t'-z) u_{-1}(t-z) X_{\text{eff}}(z) dz , \quad (6)$$

where $i=1, \dots, N$ and $-\infty < t' \leq t$.

In (6) $X_{\text{eff}}(z)$ is the effective input to the filter given by (1-33)

$$X_{\text{eff}}(z) = \frac{2}{N_0} \beta_c \{ P \sin[x(z) - \hat{x}(z)] + \sqrt{P} n_2(z) \sin \hat{x}(z) + \sqrt{P} n_1(z) \cos \hat{x}(z) \} . \quad (7)$$

The two terms n_1 and n_2 are derived from the additive noise $n(t)$. Since $n(t)$ is assumed white with density $\frac{N_0}{2}$, n_1 , n_2 and \hat{x} are independent, and $\sin \hat{x}$ and $\cos \hat{x}$ have lowpass spectra; $n_1 \sin \hat{x} + n_2 \cos \hat{x} = n'$ is also white noise with the density $\frac{N_0}{2}$ (ref.4).

Equations (6) and (7) may be represented by the block diagram shown in Fig. 1.

Fig. 1 is similar to the lowpass equivalent model of a multi-filter phase locked loop used to obtain point estimates of phase modulation components (ref. 1, Fig. 4). There are two main problems to consider with respect to Fig. 1. First the filters in Fig. 1 have the impulse responses $K_i(t')$ for $-\infty < t' \leq t$. But since $K_i(\tau)$ is an even function of τ , the filter response at t' to an impulse applied at z can be nonzero when $t > z > t'$. This implies that the N loop filters in Fig. 1 are unrealizable and that the MAP interval estimator cannot be constructed. Since $\lim_{\tau \rightarrow \pm\infty} K_i(\tau) = 0$ for the $a_i(t)$ of interest, one might consider introducing time delay into the unrealizable filters to get realizable approximations for them. Unfortunately the unrealizable filters are present in a feedback path, and this means that time delay cannot be tolerated. The second problem is to derive from Fig. 1 an optimum point estimator for the vector $\underline{a}(t)$ that gives the MMSE estimate.

2.3 A Realizable Approximation of the Optimum Demodulator

Let each unrealizable filter $K_i(\tau)$ be replaced by a realizable filter $h_{ri}(\tau)$ interior to the loop and an unrealizable filter $h_{ui}(\tau)$ exterior to the loop as shown in Fig. 2. Since $h_{ui}(\tau)$ is exterior to the feedback path, time delay can be introduced to get a realizable equivalent with delay for $h_{ui}(\tau)$. The model in Fig. 2 is an approximation of the model in Fig. 1. Thus

the estimates of $a_i(t)$ are shown as $\tilde{a}_i(t)$ in Fig.2 rather than $\hat{a}_i(t)$ as in Fig.1. For Fig.2 the reference is

$$\tilde{x}(t) = \sum_{i=1}^N \tilde{a}_{ri}(t) . \quad (8)$$

This does not equal the sum of the $\tilde{a}_i(t)$ in general since the $\tilde{a}_i(t)$ are obtained by filtering the $\tilde{a}_{ri}(t)$ with delay. If $\tilde{x}(t)$ is a sufficiently close estimate of $x(t)$ so that $\sin[x(t)-\tilde{x}(t)] \approx x(t)-\tilde{x}(t)$ most of the time, the system in Fig.2 is approximately linear. If the sine operation can be replaced by its argument (see Appendix II, Equation (2-2)) the mean square errors in making point estimates of $x(t)$ and $a_i(t)$, $i=1, \dots, N$, at time t given $r(\tau)$, $-\infty < \tau \leq t$, can be found for any $h_{ri}(\tau)$ and $h_{ui}(\tau)$ selected. If these $2N$ filters are derived by first finding the optimum linear MMSE transfer functions from $x(t)$ to $\tilde{x}(t)$ and $x(t)$ to $\tilde{a}_i(t)$, $i=1, \dots, N$, using Wiener-Hopf integral equations; the mean square errors in estimating $x(t)$ and $a_i(t)$ will be the minimum possible for the structure in Fig.2.

A lower bound $B(\underline{a}(t))$ on mean square error in estimating $\underline{a}(t)$ given $r(\tau)$, $-\infty < \tau \leq t$, can be found for the class of all possible point estimators of $\underline{a}(t)$ (see Appendix II). If the input SNR is sufficiently large such that the linearity condition holds in Fig.2, and if $h_{ri}(\tau)$ and $h_{ui}(\tau)$, $i=1, \dots, N$, are derived using Wiener-Hopf integral equation solutions in Fig.2; the error $E[(\underline{a}(t)-\tilde{\underline{a}}(t))^T(\underline{a}(t)-\tilde{\underline{a}}(t))] = B(\underline{a}(t))$. Therefore, for

large SNR into the demodulator the realizable approximation shown in Fig.2 is the optimum point estimator of $\underline{a}(t)$ in the MMSE sense.

2.4 Derivation of Optimum h_{ri}

If h_{ri} , $i=1, \dots, N$ are chosen to make $\tilde{x}(t)$ the linear MMSE estimate of $x(t)$ given $x(\tau)$ and $n'(\tau)$ for $-\infty < \tau \leq t$; it is assured that the linear assumption for Fig.2 is justified for sufficiently large SNR at the demodulator input. When $\sin[x(t) - \tilde{x}(t)]$ can be replaced by $x(t) - \tilde{x}(t)$ in Fig.2, the white noise $n'(t)$ can be transferred to the input as a white noise added to $x(t)$. This translated noise is denoted by $n''(t)$, and has the two sided power spectral density $N'' = N_0 / 2P \beta_C^2$ watts/Hz. The linear relationship between $x(t) + n''(t)$ and $\tilde{x}(t)$ is shown in Fig.3. The parallel combination of h_{ri} , $i=1, \dots, N$, is defined by $f_{ol}(t)$. If $h_{ol}(t)$ defines the linear realizable filter that gives the MMSE estimate of $x(t)$ given $x(\tau) + n''(\tau)$, $-\infty < \tau \leq t$; then the optimum $f_{ol}(t)$ follows from

$$K F_{ol}(j\omega) = H_{ol}(j\omega) / [1 - H_{ol}(j\omega)] \tag{9}$$

where F_{ol} and H_{ol} are the Fourier transforms of f_{ol} and h_{ol} , respectively, and $K = 2P \beta_C^2 / N_0$. Since $f_{ol} = \sum_{i=1}^N h_{ri}$,

$$\sum_{i=1}^N H_{ri}(j\omega) = K^{-1} H_{ol}(j\omega) / [1 - H_{ol}(j\omega)] \tag{10}$$

If each $a_i(t)$ has a rational power spectrum, it is of the form

$$S_i(\omega) = |N_i(\omega)|^2 / |D_i(\omega)|^2 \quad (11)$$

where N_i and D_i are polynomials in ω with real coefficients.

Since $x(t)$ is the sum of the independent components $a_i(t)$, $i=1, \dots, N$; the spectrum of $x(t)$ is just

$$S_x(\omega) = \sum_{i=1}^N |N_i|^2 / |D_i|^2 \quad (12)$$

The optimum realizable linear filter $h_{o\ell}$ is the solution of the Wiener-Hopf equation (ref.6, sec.5-5, eq.5.73)

$$R_x(\tau) = N'' h_{o\ell}(\tau) + \int_0^{+\infty} h_{o\ell}(z) R_x(\tau-z) dz, \quad 0 \leq \tau \quad (13)$$

For the rational spectra $S_i(\omega)$ of interest, the solution of (13) is

$$H_{o\ell}(j\omega) = 1 - 1/[1 + S_x(\omega)/N'']^+ \quad (14)$$

where $[\quad]^+$ represents the upper ω -plane poles and zeros of the rational function within the brackets (ref.6, sec.5.6, eq.5.99). Then if (14) is substituted in (10)

$$\sum_{i=1}^N H_{ri}(j\omega) = N'' [[1 + S_x(\omega)/N'']^+ - 1] \quad (15)$$

If $D_i(\omega)$ and $N_i(\omega)$ yield the upper ω -plane poles and zeros of $S_i(\omega)$ while $D_i^*(\omega)$ and $N_i^*(\omega)$ are their conjugates, respectively, then

$$\begin{aligned} \sum_{i=1}^N H_{ri}(j\omega) &= N^n \left[\left[\prod_i^N |D_i|^2 + \sum_i^N |N_i|^2 \cdot \prod_{i \neq j}^N |D_j|^2 \right]^+ \right. \\ &\quad \left. - \prod_i^N D_i \right] / \prod_i^N D_i \\ &= \sum_{i=1}^N k_i(\omega) / D_i(\omega) , \end{aligned} \tag{16}$$

where a partial fraction expansion is used to get the second equality, and $[|D_i|^2]^+ = [D_i(\omega)D_i^*(\omega)]^+ = D_i(\omega)$. For the MMSE estimate of $x(t)$ using a realizable linear filter, the choice of H_{ri} $i=1, \dots, N$, are arbitrary as long as the sum satisfies (16). The logical choice for each H_{ri} is $H_{ri}(j\omega) = k_i(\omega) / D_i(\omega)$. That is, the i^{th} filter corresponds to the poles of the i^{th} component spectrum of $S_x(\omega)$.

2.5 Derivation of Optimum h_{ui}

If the demodulator input SNR is sufficiently large, $\sin[x-\tilde{x}] \approx x-\tilde{x}$ and the system in Fig.2 can be replaced by that of Fig.4. The function of the system reduces to estimating each $a_i(t)$ from the sum $a_i(t) + n_{si}(t) + n''(t)$, where $n_{si}(t) = \sum_{j=1, j \neq i}^N a_j(t)$ may now be considered as an additional noise term added to the

white noise $n''(t)$. Since a_i , $i=1, \dots, N$, and $n''(t)$ are all Gaussian processes, the optimum filter that gives the MMSE estimate of $a_i(t)$ is linear (ref.4, sec.6.1, prop.7). This filter will be defined by the impulse response $h_{oi}(t)$; or, equivalently, by the Fourier transform $H_{oi}(j\omega)$ of $h_{oi}(t)$. If $h_{oi}(t)$ is allowed to be unrealizable for the moment, the optimum estimator of $a_i(t)$ is (ref.4, eq.119)

$$H_{oi}^u(j\omega) = S_i(\omega) / \left[N'' + \sum_{i=1}^N S_i(\omega) \right] \quad (17)$$

The transfer function from the input of Fig.4 to $\tilde{a}_{ri}(t)$ is defined by

$$H_i(j\omega) = \tilde{A}_{ri}(j\omega) / X(j\omega) \quad (18)$$

This transfer function is derived in Appendix III in terms of the transfer functions $H_{ri}(j\omega)$, $i=1, \dots, N$. The result is

$$H_i(j\omega) = K H_{ri}(j\omega) / \left[1 + K \sum_{i=1}^N H_{ri}(j\omega) \right] \quad (19)$$

for each $i=1, \dots, N$, where $K=1/N''$. Since $\tilde{a}_i(t)$ is the response of the filter $h_{ui}(t)$ to the excitation $\tilde{a}_{ri}(t)$,

$$H_{oi}(j\omega) = H_{ui}(j\omega) \cdot H_i(j\omega)$$

or

$$H_{ui}(j\omega) = H_{oi}(j\omega)/H_i(j\omega) \quad (20)$$

This is the desired transfer function of the optimum filter $h_{ui}(t)$ for each $i=1, \dots, N$. The filter is unrealizable when $H_{oi}(j\omega)$ is given by (17). Since the filters $h_{ri}(t)$ are realizable, $H_i(j\omega)$ is the transfer function of a realizable filter. Substituting (15) through (19) into (20) gives

$$H_{ui}(j\omega) = \frac{S_i(\omega) D_i(\omega)}{k_i(\omega) [1 + S_x(\omega)/N]^*} \quad (21)$$

where $D_i(\omega)/k_i(\omega)$ follows from the partial fraction expansion (16) and $[\quad]^*$ is the complex conjugate of $[\quad]^+$.

If a delay $\delta > 0$ is introduced in each post loop filter (21) the transfer function becomes $H_{ui}(j\omega)\exp[-j\omega\delta]$. In the time domain $h_{ui}(t)$ becomes $h_{ui}(t-\delta)$ and $\tilde{a}_i(t)$ becomes $\tilde{a}_i(t-\delta)$. The impulse response $h_{ui}(t)$ can be nonzero for negative t but $\lim_{t \rightarrow -\infty} h_{ui}(t) = 0$ may be assumed. Then if δ is sufficiently large, $h_{ui}(t-\delta) \approx 0$ for all $t < 0$; and the filter with the impulse response $h_{ui}(t-\delta)$ can be assumed realizable. The advantage of using delay to get realizable filters from (21) is that the errors in estimating $a_i(t)$, $i=1, \dots, N$, are the same as for the unrealizable filters. If $H_{oi}(j\omega)$ had been restrained to be realizable, then (20) would give a realizable filter for each i and there would be no need for time delay. However, the errors in estimating the $a_i(t)$ would then be increased.

2.6 MMSE In Estimating $x(t)$ And $a_i(t)$

The error in estimating $x(t)$ from $x(\tau)+n''(\tau)$, $-\infty < \tau \leq t$, is given by (ref.6, eq.5.100)

$$\sigma_o^2 = \frac{N''}{2\pi} \int_{-\infty}^{+\infty} \ln[1 + S_x(\omega)/N''] d\omega \quad (22)$$

where the optimum filter has the transfer function H_{ol} in (14).

The error in estimating $a_i(t)$ given $x(\tau)+n''(\tau)$, $-\infty < \tau \leq t$, is (ref.6, eq.5.98)

$$\sigma_{oi}^2 = \frac{1}{2\pi} \int_{-\infty}^{\infty} \frac{S_i(\omega) [S_x(\omega) - S_i(\omega) + N'']}{S_x(\omega) + N''} d\omega \quad (23)$$

when the time delay $\delta \rightarrow +\infty$. The error in (23) is just the error achieved when an optimum unrealizable filter is used to estimate $a_i(t)$ from $x(\tau)+n''(\tau)$, $-\infty < \tau < +\infty$. It is usually acceptable to let δ be several times greater than the largest time constant of the correlation functions $K_i(\tau)$, $i=1, \dots, N$.

2.7 Examples Where $N=2$ And $S_1(\omega) S_2(\omega) \neq 0$

In Appendix IV an example is discussed where $S_x(\omega) = S_1(\omega) + S_2(\omega)$ with

$$S_1(\omega) = 2a_1 p_1 / [\omega^2 + p_1^2] \quad (24)$$

and

$$S_2(\omega) = a_2 p_2 / [(\omega + \omega_2)^2 + p_2^2] + a_2 p_2 / [(\omega - \omega_2)^2 + p_2^2]$$

The filters $H_{ri}(j\omega)$ and $H_{ui}(j\omega)$ are derived for $i=1,2$ and expressions for the errors σ_{o1}^2 , σ_{o2}^2 and σ_o^2 are found for the optimum estimation of $a_1(t)$ and $a_2(t)$ with delay and of $x(t)$ with no delay. The input used to estimate $a_1(t)$, $a_2(t)$ and $x(t)$ was $x(\tau)+n''(\tau)$, $-\infty < \tau \leq t$.

Graphs of S_1 , S_2 and N'' are shown superimposed in Fig.5 for the values $a_1=p_1=1$, $a_2=p_2=0.2$, $N''=0.1$ and $\omega_2=9.8$. Also shown in Fig.5 is another possible $S_1(\omega)$ of the form $C \sin^2(A\omega/2)/(A\omega/2)^2$ where A and C are positive constants. For $A=C=0.9$ the total area over $(-\infty < \omega < +\infty)$ under the two $S_1(\omega)$ curves is equal to $a_1=1$, and the area over the interval $(-7 < \omega < +7)$ is 0.91. The 91% power frequency occurs at the first null of the function $C \sin^2(\omega A/2)/(\omega A/2)^2$. Using alternately the rational and irrational functions for $S_1(\omega)$ as shown in Fig.5, the errors σ_{o1}^2 , σ_{o2}^2 and σ_o^2 were computed using (22) and (23). The computations were made for a range of the normalized white noise N'' and various center frequencies ω_2 of $S_2(\omega)$. The range of N'' used varied with ω_2 . For each ω_2 , N'' was bounded by N_{\max} and $0.01 N_{\max}$ where N_{\max} gave $\sigma_o^2=0.25$. This value of loop error was taken to be the threshold of linear operation for the loop as N'' increased.

Graphs of a_1/σ_{o1}^2 , a_2/σ_{o2}^2 and σ_o^2 are plotted in Figs.6-8, respectively, for the case of $S_1(\omega)$ and $S_2(\omega)$ given in (24) and the specific a_1 , a_2 , p_1 and p_2 shown in Fig.5. Since a_1 and a_2 equal the average powers of the modulating signals $a_1(t)$ and $a_2(t)$, and since σ_{o1}^2 and σ_{o2}^2 are the mean square errors in estimating $a_1(t)$ and $a_2(t)$; the ordinates in Figs.6 and 7 may be defined

as the output signal-to-noise ratios (SNR's) of the demodulators for $a_1(t)$ and $a_2(t)$, respectively. Similar graphs are given in Figs.9-11 for $C/A\sigma_{O1}^2$, a_2/σ_{O2}^2 but σ_O^2 where the irrational function shown in Fig.5 is used for $S_1(\omega)$ and $S_2(\omega)$ is unchanged. Since C/A is the average power of $a_1(t)$ for the case of the irrational $S_1(\omega)$, the ordinates in Figs.9 and 10 are again the output SNR's of the demodulators for $a_1(t)$ and $a_2(t)$. All functions in Figs.6-11 are plotted with respect to $1/N''$. Hence since $N''=N_O/2P \beta_c$ the demodulator output SNR's are monotonically increasing functions of the input signal power-to-noise power spectral density ratio $2P/N_O$ for a fixed carrier phase modulation index β_c . For given input signal power P and noise density $N_O/2$, the output SNR's also increase with β_c . However, any improvement gained by increasing β_c is accompanied by an increase in the bandwidth around ω_c needed to transmit $s(t, \underline{a}(t))$ with fidelity. Hence, the size of β_c is bounded by bandwidth restraints.

The rational $S_1(\omega)$ considered is a decreasing function of ω . Then as the center frequency ω_2 of $S_2(\omega)$ is increased and all other parameters are fixed, the errors σ_{O1}^2 and σ_{O2}^2 must decrease for any given N'' . This follows since the interference between $a_1(t)$ and $a_2(t)$ decreases with increasing $\omega_2 > 0$. However, since the irrational $S_1(\omega)$ considered has periodic nulls the functions σ_{O1}^2 and σ_{O2}^2 oscillate as ω_2 increases from zero. These observations are borne out by the graphs in Figs.6,7,9 and 10. It is obvious that the estimations of $a_1(t)$ and $a_2(t)$ are best in the MMSE sense when their mutual interference is minimized. For the

rational $S_1(\omega)$ example the best performance will occur when $\omega_2 \rightarrow \infty$. For the irrational $S_1(\omega)$ example the best performance will also occur as $\omega_2 \rightarrow \infty$, but there are locally optimum values of ω_2 around the nulls of $S_1(\omega)$. For the case of two subcarrier signals it follows from (23) that σ_{O1}^2 and σ_{O2}^2 are simultaneously minimized by minimizing the integral of $S_1(\omega)S_2(\omega)/[S_1(\omega)+S_2(\omega)+N]$. This integral is minimum, of course, when $S_1(\omega)$ and $S_2(\omega)$ are orthogonal in frequency.

4.0 CONCLUSIONS

An asymptotically optimum (A.O.) phase demodulator has been derived for recovering MMSE estimates of interfering frequency multiplexed subcarrier signals. The demodulator is A.O. since it becomes the best as the input-carrier-power to input-noise-spectral-density $2P/N_0$ becomes large. In practice, as $2P/N_0$ increases from zero, a value is reached called the threshold above which the A.O. demodulator applies. This threshold phenomenon is characteristic of phase or frequency modulation and results from the nonlinear nature of the modulation. The threshold is easily derived from an upper bound placed on the phase error σ_0^2 of equation (22).

Components of the A.O. demodulator are derived as optimum filter transfer functions $H_{ri}(j\omega)$ and $H_{ui}(j\omega)$ that depend on the particular forms of the subcarrier signal spectra and the value of $2P/N_0$. The impulse functions $h_{ri}(t)$ and $h_{ui}(t)$, $i=1, \dots, N$, for the filters in the A.O. demodulator of Fig. 4

are the inverse Fourier transforms of $H_{ri}(j\omega)$ and $H_{ui}(j\omega)$. The interference between subcarrier signals due to overlap in their power spectra in the subcarrier band complicates the derivation of the A.O. demodulator components, but only moderately. The forms of these transfer functions are given in (16) and (21).

Since the filters $h_{ri}(t)$, $i=1, \dots, N$, are interior to the feedback loop in Fig. 4, no time delay can be tolerated in them, and they are realized as optimum filters that process inputs up to t for MMSE estimates at t . But the filters $h_{ui}(t)$, $i=1, \dots, N$, are post loop, and the subcarrier signal estimates at the outputs of the filters can be improved by introducing time delay into $h_{ui}(t)$, $i=1, \dots, N$. As the time delay is increased, the subcarrier signal estimation errors approach the lower bounds in (23). The filters to be used in the A.O. demodulator are all realizable, but time delay is necessary for the $h_{ui}(t)$, $i=1, \dots, N$, in order to achieve the irreducible errors in (23). If time delay cannot be tolerated, the filters $h_{ui}(t)$, $i=1, \dots, N$, are the realizable linear filters that give the MMSE estimates of the subcarrier signals at time t given inputs at these filters for all time up to t . The estimation errors for this case follow from (22).

The development through section 2.6 applies to any N subcarrier signals that may be interfering, but are statistically independent wide sense stationary Gaussian processes with zero means.

Examples are discussed in section 2.7 that demonstrate the theory. For the case of $N=2$ and overlapping subcarrier signal spectra, the equations (22) and (23) are applied to find the total loop tracking error σ_0^2 and the MMSE's σ_{01}^2 and σ_{02}^2 in estimating the two subcarrier signals. The performance of the A.O. demodulator is measured in terms of σ_0^2 and the signal-to-noise ratio (SNR) defined to be the ratio of subcarrier-signal-variance to subcarrier-estimation-error. The two SNR's and σ_0^2 are plotted vs. $\beta_c(2P/N_0)$ where β_c is the carrier phase modulation index common to all subcarrier signals. The position in frequency of the two subcarrier signals in the subcarrier band is used as a parameter. As $2P/N_0$ decreases with β_c fixed, a line is reached where $\sigma_0^2 = 0.25$. For $2P/N_0$ above this line $\sigma_0^2 < 0.25$ and the A.O. demodulator is applicable. The line for $\sigma_0^2 = 0.25$ is defined to be the threshold of the A.O. demodulator.

In the examples one subcarrier signal has a broadband video spectrum while the other has a narrow bandpass spectrum centered about a subcarrier frequency. In one case the broadband video spectrum is $C \sin^2(A\omega/2) / (A\omega/2)^2$ with alternating peaks and valleys similar to the spectrum of a TV signal. As the center frequency of the narrow bandpass signal is shifted, the oscillations in the performance of the the demodulator are determined. More exact but tractable mathematical models exist for the spectrum of stationary picture TV signals (ref. 9).

These spectra can be used in the equations derived in this memorandum to compute performance of the A.O. demodulator for a stationary TV signal with an interfering voice subcarrier signal.

4.0 REMARKS

This memorandum has addressed the particular problem of demodulating interfering subcarrier signals phase modulated directly onto the carrier. The problem of demodulating interfering subcarrier signals frequency modulated directly onto the carrier can be solved by a parallel treatment. For the case of multilevel phase or frequency modulation of a carrier, the techniques of this memorandum can be applied to get an A.O. demodulator for the subcarrier signals in the MMSE sense. However, there are mathematical difficulties in evaluating the performance of these demodulators when multilevel modulation is used and the subcarrier signals are interfering. A complete solution of this more difficult problem is not known at this time.

W. D. Wynn

W. D. Wynn

2034-WDW-CS

Attachments
Figures 1-15

BELLCOMM, INC.

REFERENCES

1. Wynn, W. D., "Optimum and Suboptimum Demodulators for FM Signals with Multiple Subcarriers", TM-69-2034-7, Bellcomm, Inc., Washington, D. C., 1969.
2. "Proceedings Of The Apollo Unified S-Band Technical Conference", NASA SP-87, Goddard Space Flight Center, July 1965.
3. Lee, S. Y., "A Computer Method for the Determination of Rational Functions", TM-69-1033-4, Bellcomm, Inc., Washington, D. C., 1969.
4. VanTrees, H. L., Detection, Estimation, and Modulation Theory, Part I, John Wiley, New York, 1968.
5. Snyder, D. L., The State-Variable Approach To Continuous Estimation, Monograph 51, The M.I.T. Press, Cambridge, Massachusetts, 1969.
6. Viterbi, A. J., Principles of Coherent Communication, McGraw-Hill, New York, 1966.
7. Papoulis, Athanasios, Probability, Random Variables, and Stochastic Processes, McGraw-Hill Book Company, New York, 1965.
8. Wylie, C. R., Jr., Advanced Engineering Mathematics, McGraw-Hill Book Company, New York, 1951.
9. Franks, L. E., "A Model for the Random Video Process," Bell System Technical Journal, Vol. XLV, No. 4, April, 1966.

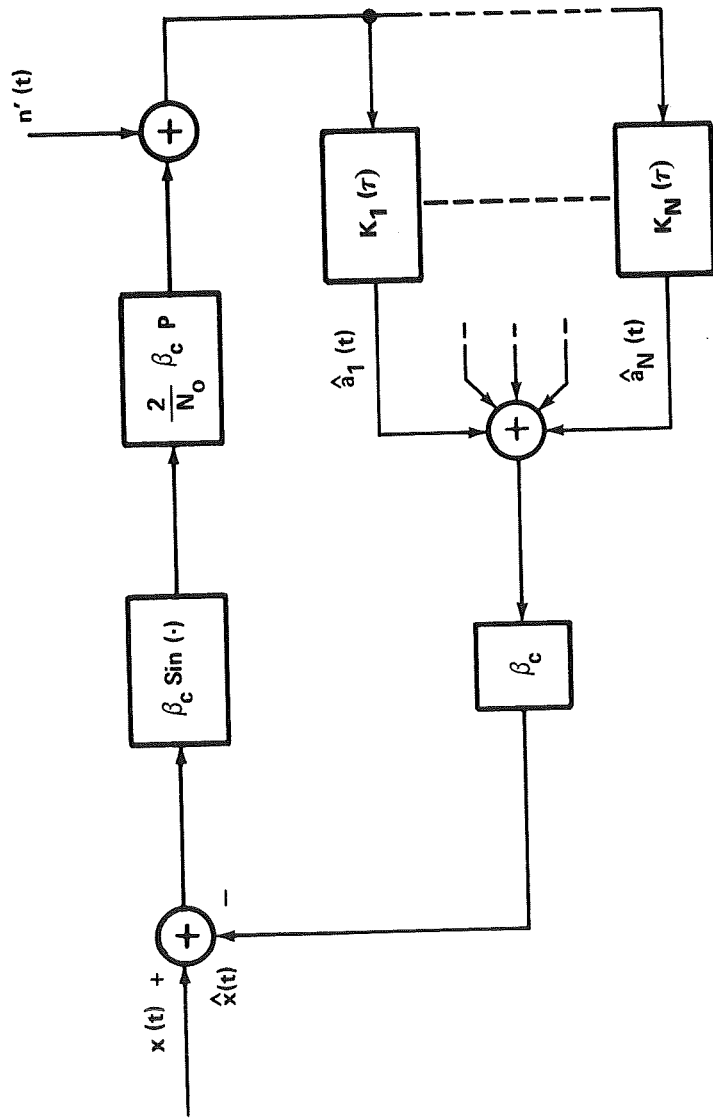


FIGURE 1 - LOW FREQUENCY EQUIVALENT MAP INTERVAL ESTIMATOR FOR DEMODULATING $a_i(t)$, $i = 1, \dots, N$.

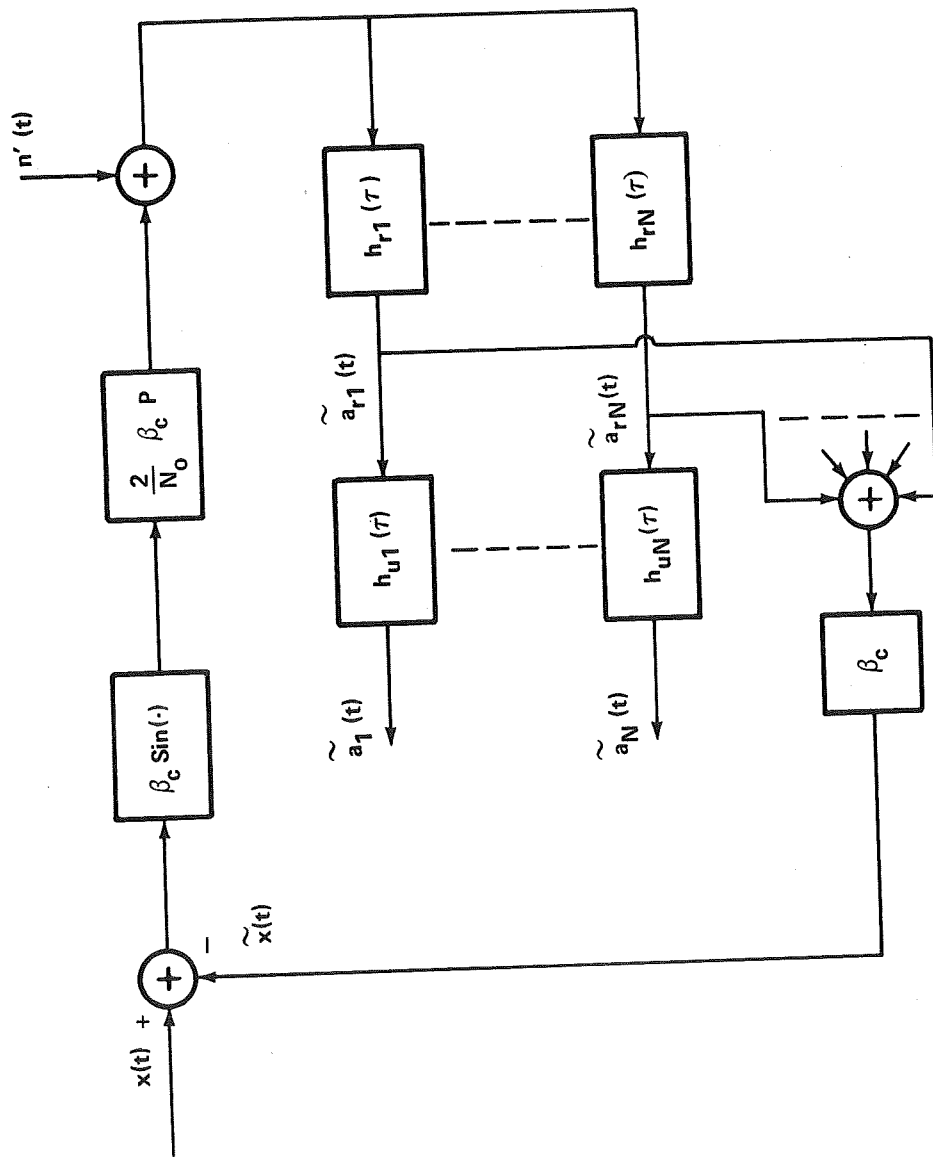


FIGURE 2 - REALIZABLE APPROXIMATION OF THE LOW FREQUENCY EQUIVALENT MAP INTERVAL ESTIMATOR FOR DEMODULATING $a_i(t)$, $i=1, \dots, N$.

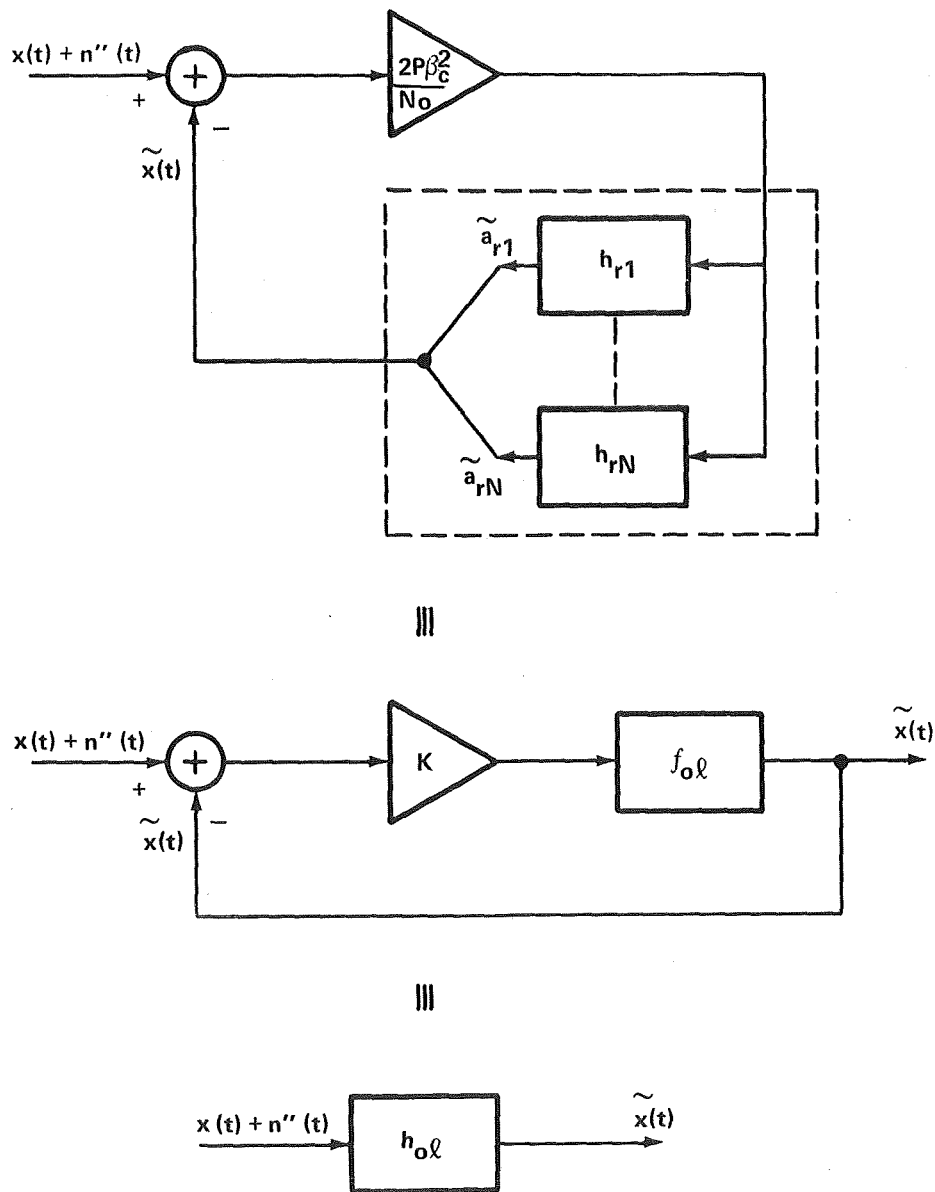


FIGURE 3 - THREE EQUIVALENT REPRESENTATIONS OF THE LINEAR APPROXIMATION OF FIGURE 2 FOR ESTIMATION OF $x(t)$ GIVEN $x(t) + n''(t)$.

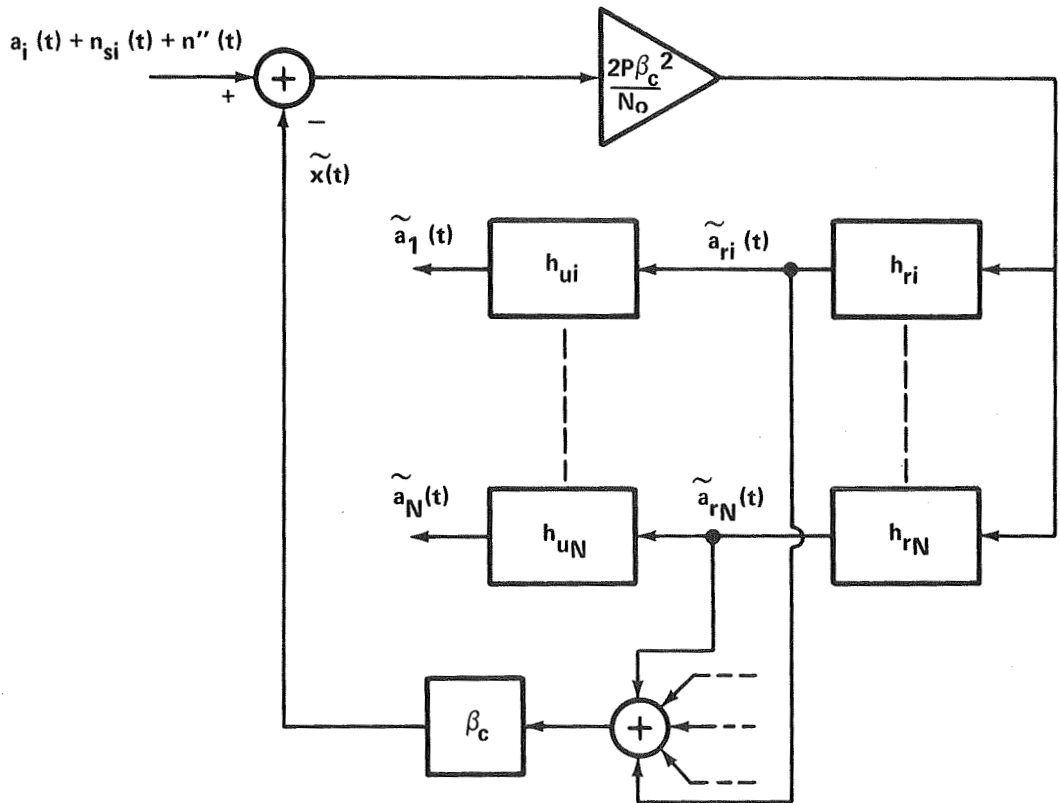


FIGURE 4 - THE LINEAR APPROXIMATION OF THE SYSTEM IN FIGURE 2 FOR ESTIMATING $a_i(t)$ GIVEN $a_i + n_{si} + n''$

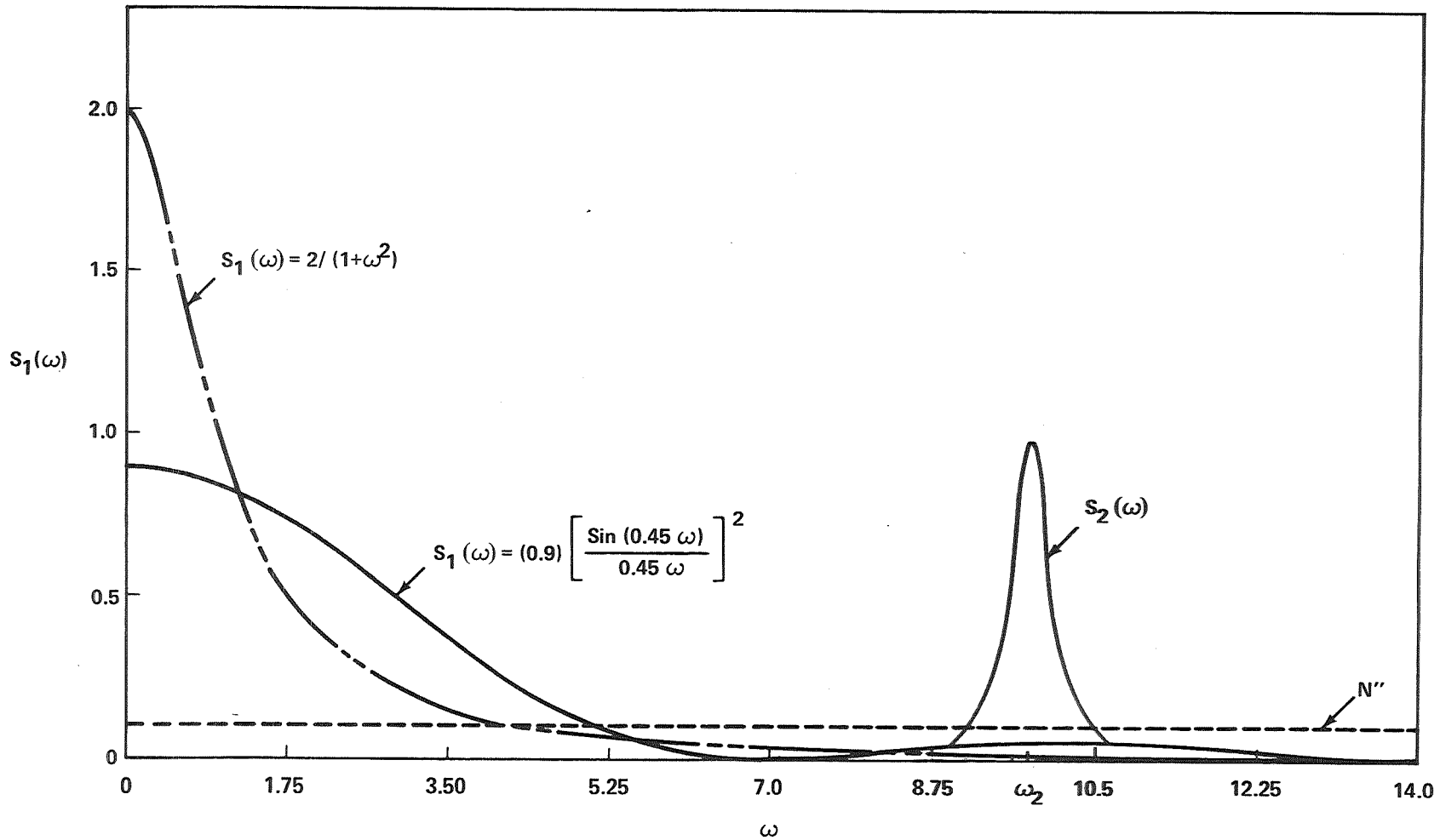


FIGURE 5 - GRAPHS OF TWO SIGNAL SPECTRA $S_1(\omega)$ WITH EQUAL TOTAL POWER AND 91% POWER FREQUENCY $\omega = 7.0$, AND THE SIGNAL SPECTRUM $S_2(\omega)$ AT A TYPICAL SUBCARRIER FREQUENCY ω_2 . ONE UNIFORM NORMALIZED NOISE DENSITY N'' IS SHOWN AS A DASHED LINE.

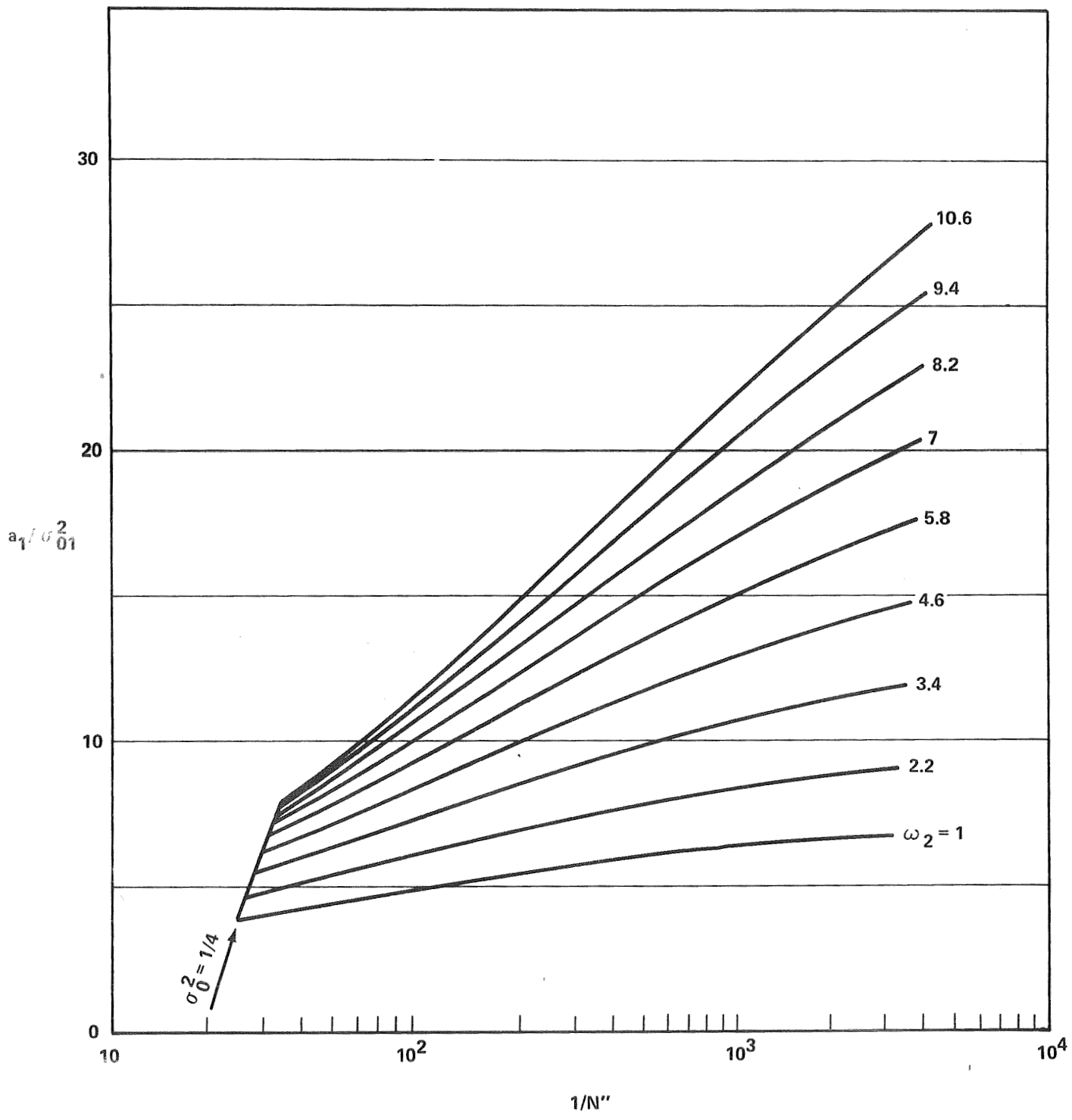


FIGURE 6 - RATIO OF SIGNAL POWER TO ESTIMATION ERROR (SNR) AT OUTPUT OF FIRST DEMODULATOR. RATIONAL $S_1(\omega)$ WITH $a_1 = p_1 = 1$; $a_2 = p_2 = 0.2$

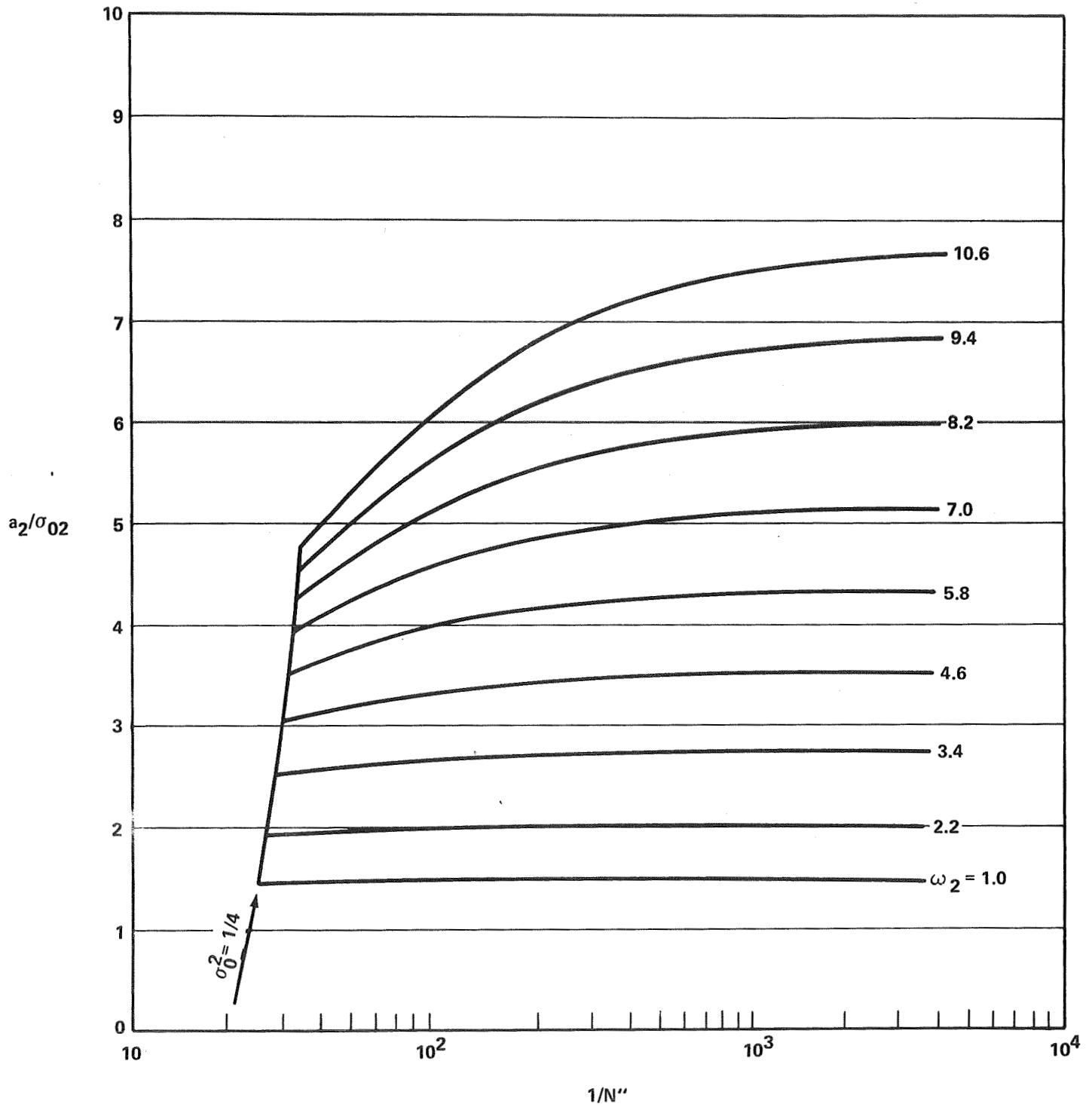


FIGURE 7 - RATIO OF SIGNAL POWER TO ESTIMATION ERROR (SNR) AT OUTPUT OF SECOND DEMODULATOR. RATIONAL $S_1(\omega)$ WITH $a_1 = p_1 = 1$; $a_2 = p_2 = 0.2$

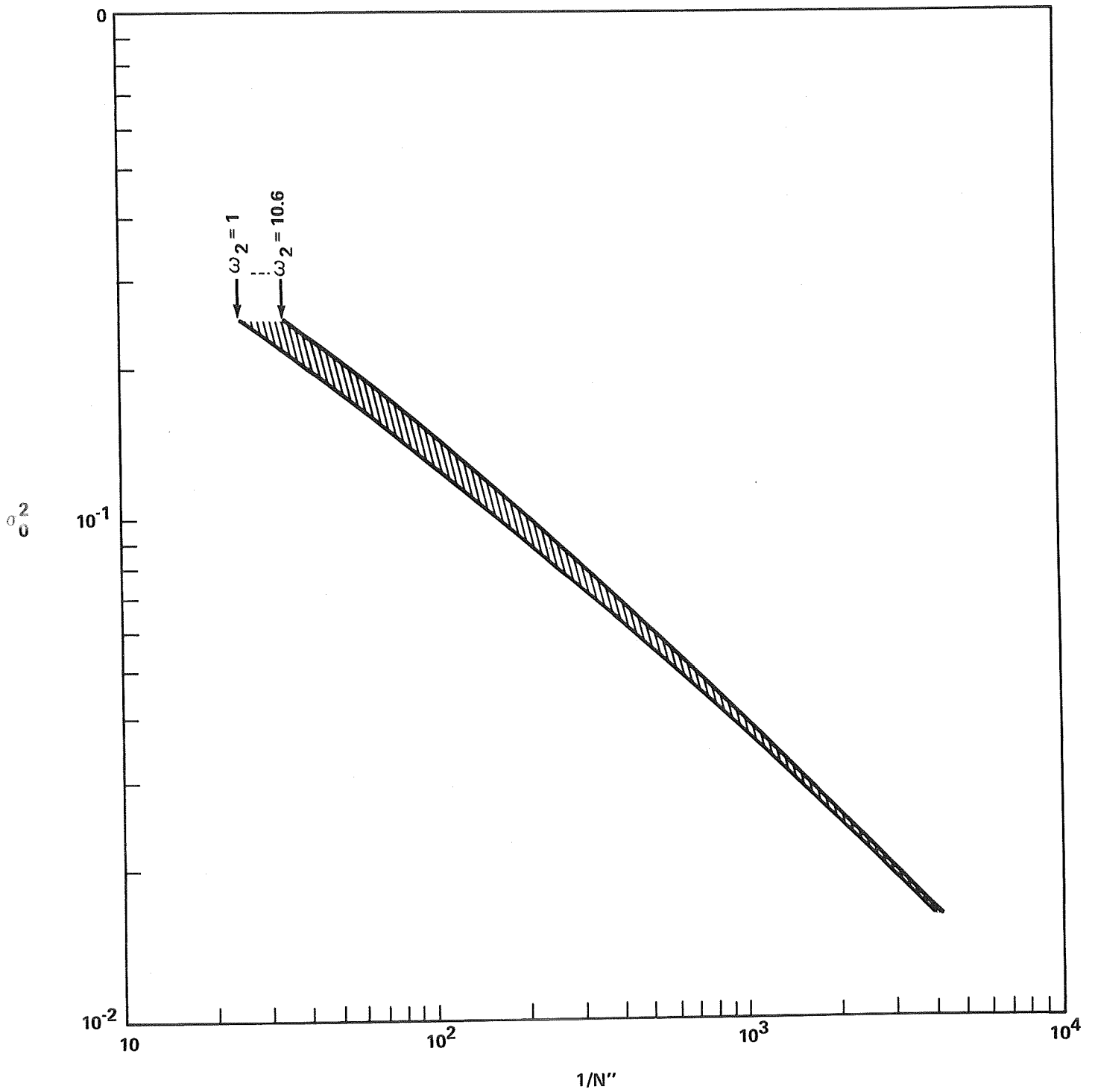


FIGURE 8:- TOTAL PLL ERROR VS. INVERSE OF NOISE DENSITY N''
 WITH PARAMETER ω_2 . RATIONAL $S_1(\omega)$ AND $a_1 = p_1 = 1$;
 $a_2 = p_2 = 0.2$

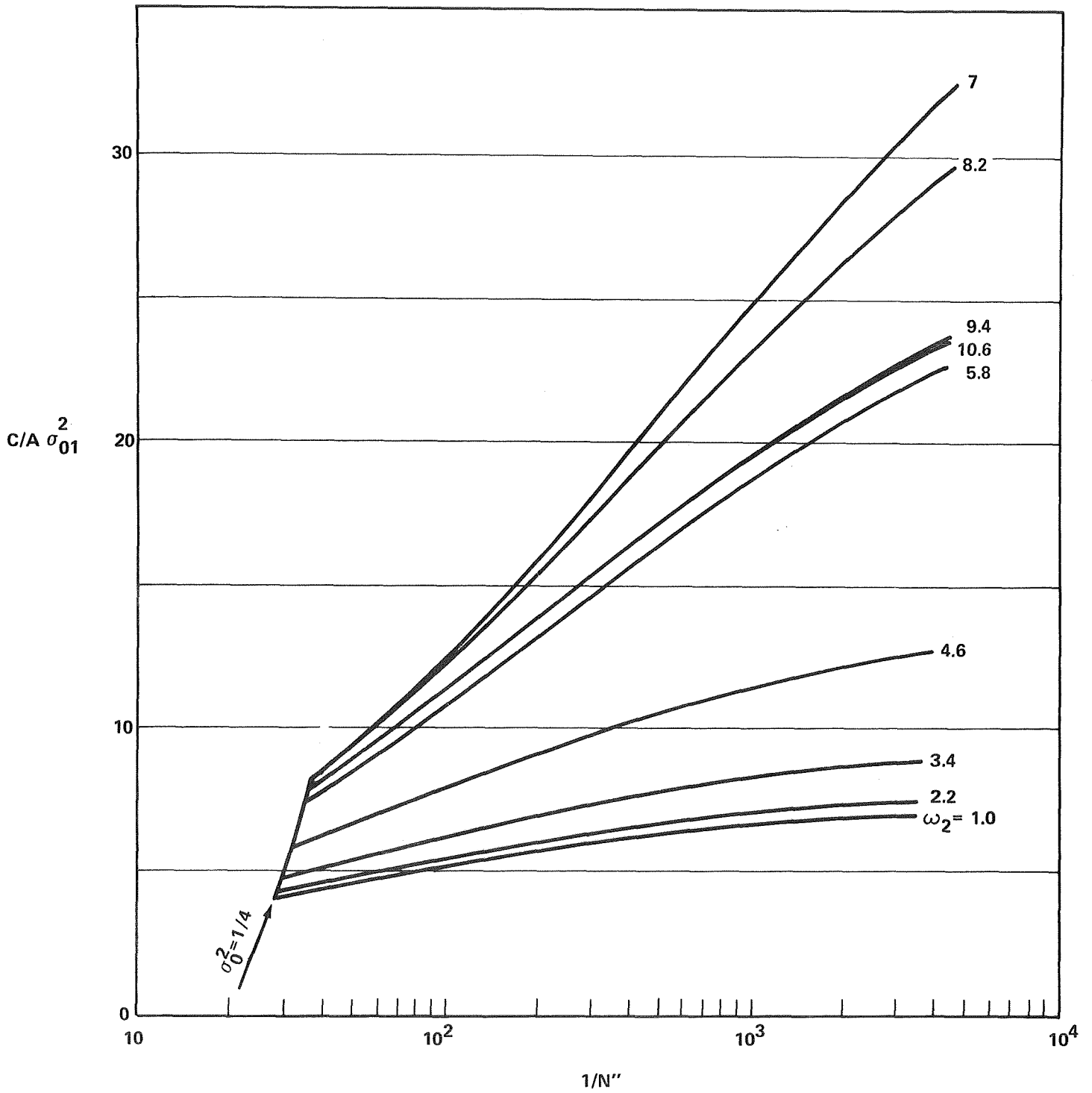


FIGURE 9 - RATIO OF SIGNAL POWER TO ESTIMATION ERROR (SNR) AT OUTPUT OF FIRST DEMODULATOR. IRRATIONAL $S_1(\omega)$ WITH $C = A = 0.9; a_2 = p_2 = 0.2$

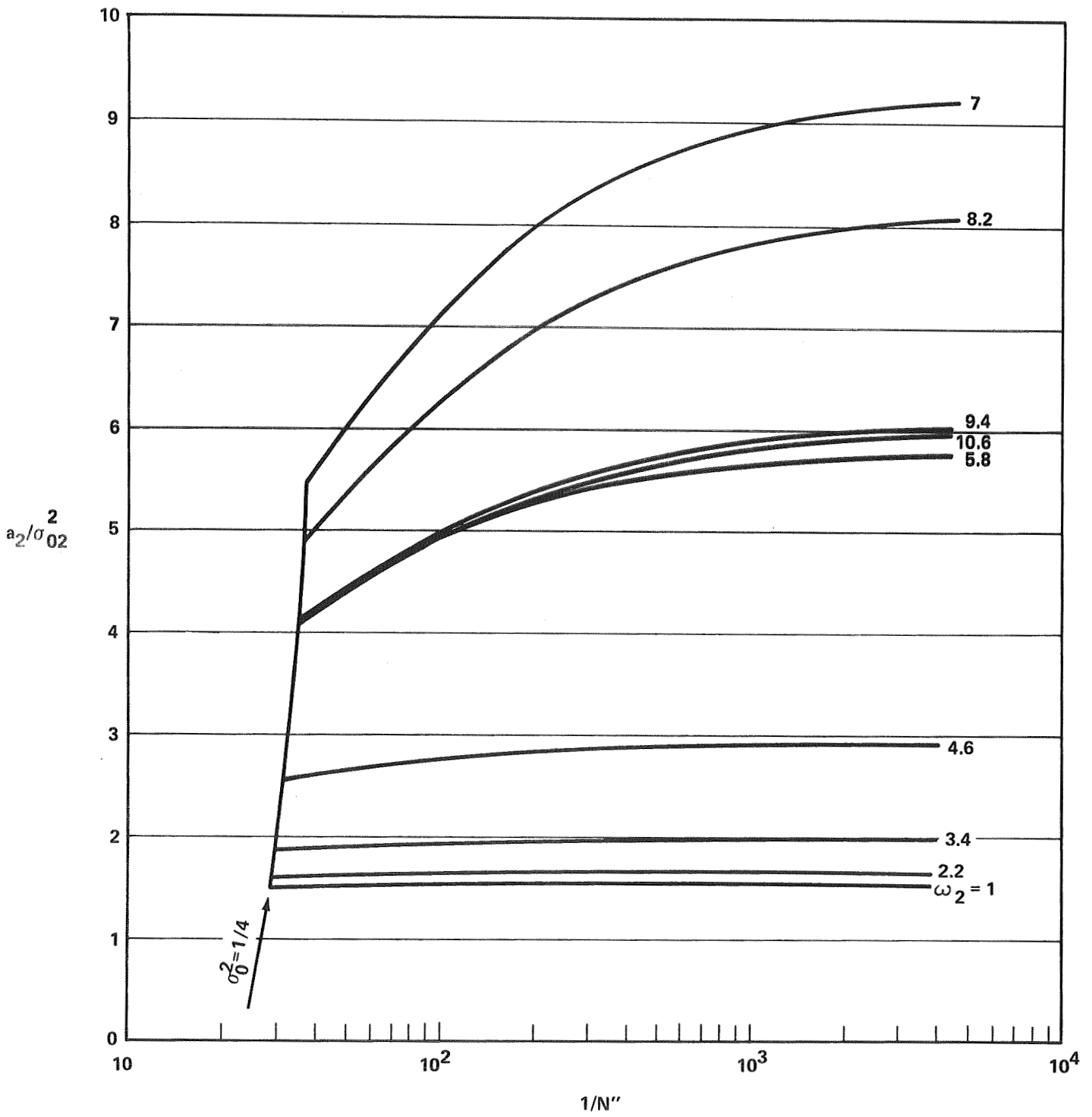


FIGURE 10 - RATIO OF SIGNAL POWER TO ESTIMATION ERROR (SNR) AT OUTPUT OF SECOND DEMODULATOR. IRRATIONAL $S_1(\omega)$ WITH $C = A = 0.9$; $a_2 = p_2 = 0.2$

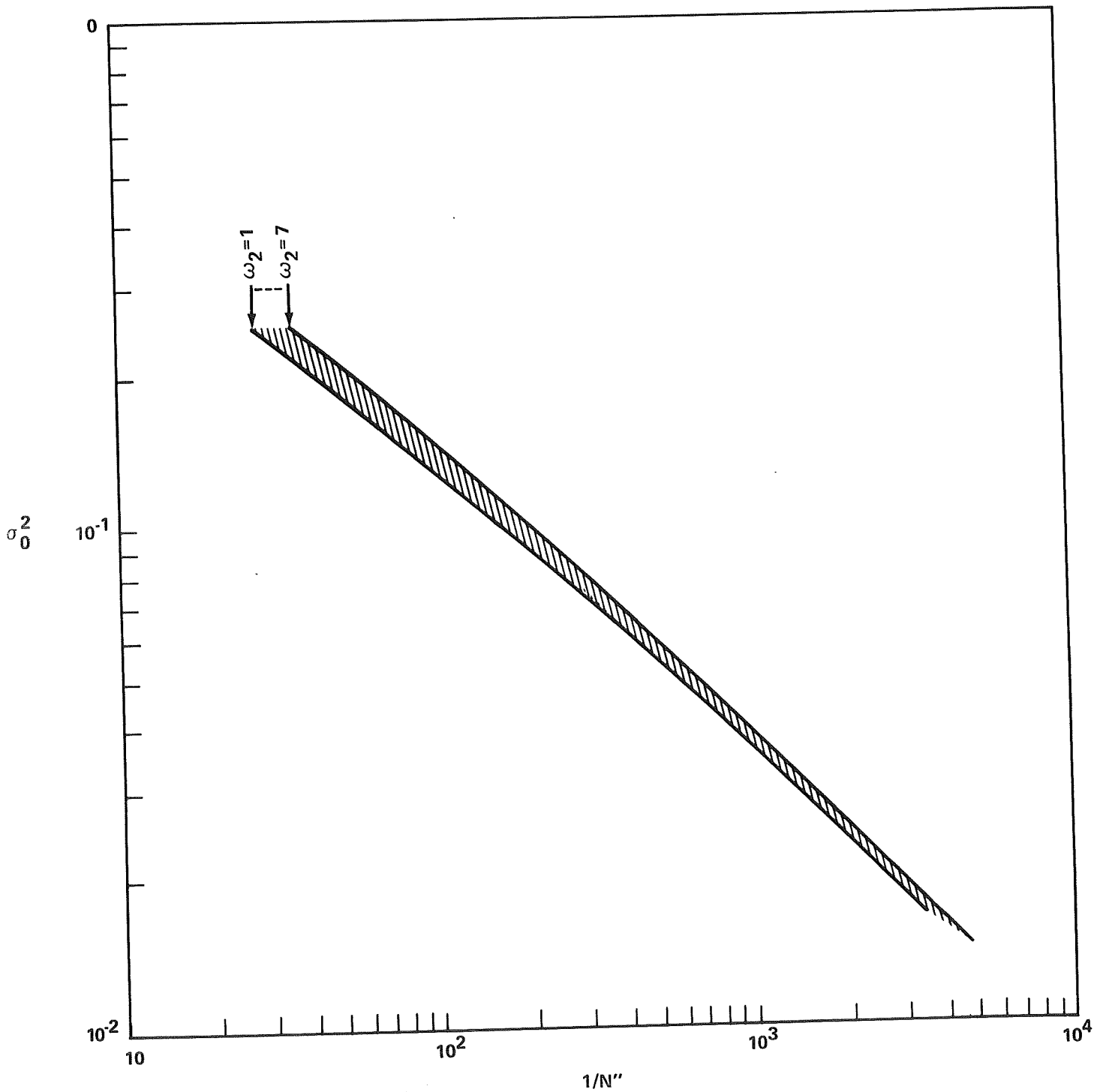


FIGURE 11 - TOTAL PLL ERROR VS. INVERSE OF NOISE DENSITY N'' WITH PARAMETER ω_2 . IRRATIONAL $S_1(\omega)$ AND $C = A = 0.9$; $a_2 = p_2 = 0.2$

APPENDIX I

Interval Estimation of Multidimensional Waveforms

The theory of interval estimation of an N dimensional waveform $\underline{a}(t)$ is discussed in reference 4, section 5.4. The purpose of this appendix is to summarize the results of reference 4, section 5.4 as they apply to the multisubcarrier phase modulated signal described in this memorandum.

Notationally, a set of N scalar time functions (messages) $a_1(\tau), \dots, a_N(\tau)$ defined on an interval $\tau \in [T_i, T_f]$ is represented by the N-vector

$$\underline{a}(\tau) = \begin{bmatrix} a_1(\tau) \\ a_2(\tau) \\ \cdot \\ \cdot \\ \cdot \\ a_N(\tau) \end{bmatrix} \quad (1-1)$$

There may be M scalar time functions (carriers) $s_1(t), s_2(t), \dots, s_M(t)$ that depend upon $\underline{a}(\tau)$ over $[T_i, T_f]$. Each member s_i should then be written as $s_i(t, \underline{a}(\tau))$, $T_i \leq t, \tau \leq T_f$. The M functions s_i can be represented as an M-vector

$$\underline{s}(t, \underline{a}(\tau)) = \begin{bmatrix} s_1(t, \underline{a}(\tau)) \\ s_2(t, \underline{a}(\tau)) \\ \cdot \\ \cdot \\ \cdot \\ s_M(t, \underline{a}(\tau)) \end{bmatrix} . \quad (1-2)$$

A simple example of (1-2) is the case of M carriers each modulated by N FM subcarrier messages. The i^{th} member of (1-2) then has the form

$$s_i(t, \underline{a}(\tau)) = \sqrt{2P} \sin \left[\omega_{ci} t + \sum_{j=1}^N d_j \int_{T_i}^t a_j(\tau) d\tau \right] . \quad (1-3)$$

If each s_i in (1-2) is transmitted over a channel that corrupts it with an additive noise $n_i(t)$, the M received signals $r_i(t)$, $i=1, \dots, M$, can be represented in vector form by

$$\underline{r}(t) = \underline{s}(t, \underline{a}(\tau)) + \underline{n}(t), \quad T_i \leq t, \tau \leq T_f, \quad (1-4)$$

where the i^{th} member of this vector equation satisfies

$$r_i(t) = s_i(t, \underline{a}(\tau)) + n_i(t), \quad T_i \leq t, \tau \leq T_f. \quad (1-5)$$

The waveform $s_i(t, \underline{a}(\tau))$ can be a nonlinear function of $\underline{a}(\tau)$ as indicated by (1-3). The significance of τ in (1-2) is that memory can exist in the operation of modulating \underline{s} by \underline{a} . Again, an example is (1-3). If there is no memory, the value of \underline{s} at

time t depends only upon t and $\underline{a}(t)$. For the no memory case $\underline{s}(t, \underline{a}(\tau)) = \underline{s}(t, \underline{a}(t))$. An example of no memory modulation is multiple subcarrier phase modulation of \underline{s} . Here each $s_i(t, \underline{a}(t))$ would be given by (1-3) if the integral were removed and replaced by $a_j(t)$.

In the following discussion of optimum interval estimators it is assumed that the messages $a_i(t)$, $i=1, \dots, N$, are sample functions from continuous, jointly Gaussian random processes. The components of $\underline{n}(t)$ are also assumed to have these properties. Under these restrictions the analysis of optimum interval estimators of \underline{a} is tractable. The covariance functions of $\underline{a}(t)$ and $\underline{n}(t)$ can be written

$$E[\underline{a}(t) \underline{a}^T(u)] = \underline{K}_{\underline{a}}(t, u) , \quad (N \times N) \quad (1-6)$$

and

$$E[\underline{n}(t) \underline{n}^T(u)] = \underline{K}_{\underline{n}}(t, u) , \quad (M \times M) \quad (1-7)$$

The element in the i^{th} row and j^{th} column of $\underline{K}_{\underline{a}}$ is $E[a_i(t) a_j(u)] = R_{ij}(t, u)$, $1 \leq i, j \leq N$. The element in the i^{th} row and j^{th} column of $\underline{K}_{\underline{n}}$ is $E[n_i(t) n_j(u)] = R_{ij}^n(t, u)$, $1 \leq i, j \leq M$. Interdependence could also exist between \underline{n} and \underline{a} , and it is possible to incorporate this generalization into the analysis, but such will not be done in this memorandum. If the elements of \underline{a} and \underline{n} have non-zero means the mathematical details are only slightly more complicated than in the case of zero means. It suffices to consider the case

of zero means for \underline{a} and \underline{n} . With these conditions the processes \underline{a} and \underline{n} are completely described by (1-6) and (1-7), respectively.

The vector random process $\underline{a}(t)$ can be expanded into the vector orthogonal series (ref. 4, section 3-7)

$$\underline{a}(t) = \text{l.i.m.}_{K \rightarrow \infty} \sum_{r=1}^K a_r \underline{\psi}_r(t), \quad T_i \leq t \leq T_f. \quad (1-8)$$

where l.i.m. means limit-in-the-mean, $\underline{\psi}_r(t)$ is a nonrandom N-vector for each r , and a_r is a scalar random variable. The vectors $\underline{\psi}_r(t)$ are vector eigenfunctions corresponding to the integral equation

$$\mu_r \underline{\psi}_r(t) = \int_{T_i}^{T_f} \underline{K}_{\underline{a}}(t,u) \underline{\psi}_r(u) du, \quad T_i \leq t \leq T_f. \quad (1-9)$$

The scalar random variables a_r are given by

$$a_r = \int_{T_i}^{T_f} \underline{\psi}_r^T(t) \underline{a}(t) dt, \quad r = 1, 2, \dots \quad (1-10)$$

Since the vector $\underline{a}(t)$ is assumed Gaussian with zero mean, a_i and a_j are statistically independent if $i \neq j$; and $E[a_i a_j] = \mu_i \delta_{ij}$ where $\delta_{ij} = 1$ for $i=j$ and zero otherwise.

One optimum interval estimate of $\underline{a}(t)$ on $[T_i, T_f]$ is the MAP estimate defined as follows. Given any integer $K > 0$, the N-vector $\underline{a}_K(t)$ is defined by

$$\underline{a}_K(t) = \sum_{r=1}^K a_r \underline{\psi}_r(t), \quad T_i \leq t \leq T_f. \quad (1-11)$$

This is the K^{th} partial sum of $\underline{a}(t)$ in (1-8), where a_r and $\underline{\psi}_r$ are derived in (1-9) and (1-10). If \underline{a}_K is substituted for \underline{a} in (1-4) there results the new M-vector equation

$$\underline{r}_K(t) = \underline{s}(t, \underline{a}_K(\tau)) + \underline{n}(t), \quad T_i \leq t \leq T_f. \quad (1-12)$$

From (1-12) a MAP estimate of the random variables a_r , $r=1, \dots, K$, can be made (ref. 4, section 4.6). With this MAP estimate denoted by \hat{a}_r , for each r , an estimate of $\underline{a}_K(t)$ in (1-11) is generated by

$$\hat{\underline{a}}_K(t) = \sum_{r=1}^K \hat{a}_r \underline{\psi}_r(t), \quad T_i \leq t \leq T_f. \quad (1-13)$$

The MAP interval estimate of $\underline{a}(t)$ on $[T_i, T_f]$ is defined by $\hat{\underline{a}}_{\text{map}}(t)$ where

$$\hat{\underline{a}}_{\text{map}}(t) = \underset{K \rightarrow \infty}{\text{l.i.m.}} \hat{\underline{a}}_K(t), \quad T_i \leq t \leq T_f. \quad (1-14)$$

When it is understood that a MAP interval estimate is being made the "map" subscript is omitted, and $\hat{\underline{a}}$ denotes (1-14). The limit (1-14) is known to satisfy the vector integral equation (1-15) for the no memory modulation case $\underline{s}(t, \underline{a}(\tau)) = \underline{s}(t, \underline{a}(t))$ (ref. 4, equation 5-160).

$$\hat{\underline{a}}(t) = \int_{T_i}^{T_f} \underline{K}_{\underline{a}}(t, z) \underline{D}(z, \hat{\underline{a}}(z)) [\underline{r}_g(z) - \underline{g}(z)] dz, \quad T_i \leq t \leq T_f. \quad (1-15)$$

Here

$$\underline{r}_g(z) = \int_{T_i}^{T_f} \underline{Q}_{\underline{n}}(z, u) \underline{r}(u) du, \quad (1-16)$$

and

$$\underline{g}(z) = \int_{T_i}^{T_f} \underline{Q}_{\underline{n}}(z, u) \underline{s}(u, \underline{a}(u)) du, \quad (1-17)$$

where $\underline{Q}_{\underline{n}}$ is defined by

$$\int_{T_i}^{T_f} \underline{K}_{\underline{n}}(t, z) \underline{Q}_{\underline{n}}(z, u) du = \delta(t-u) \underline{I}, \quad (1-18)$$

with

$$\underline{I} = \begin{bmatrix} 1 & & & 0 \\ & \cdot & & \\ & & \cdot & \\ & & & \cdot \\ 0 & & & 1 \end{bmatrix} \quad \text{and } T_i \leq t, u \leq T_f. \quad M \times M$$

Also, $\underline{D}(t, \underline{a}(t))$ is a matrix with N rows and M columns where the term in the i^{th} row and j^{th} column is $\partial s_i(t, \underline{a}(t)) / \partial a_j(t)$.

A system that performs operations on the received vector waveform $\underline{r}(t) = s(t, \underline{a}(t)) + \underline{n}(t)$, $T_i \leq t \leq T_f$, is called a MAP interval estimator of $\underline{a}(t)$ on $[T_i, T_f]$. The three equations are represented by the feedback system in Fig.12. The double lines indicate vector transfer and the sum and product are vector operations.

The particular signal demodulator investigated in this memorandum processes the waveform

$$\begin{aligned} r(\tau) &= s(\tau) + n(\tau) & (1-19) \\ &= \sqrt{2P} \sin \left[\omega_c \tau + \beta_c \sum_{i=1}^N a_i(\tau) \right] + n(\tau) , & -\infty < \tau \leq t , \end{aligned}$$

where $n(t)$ is white Gaussian noise with the two-sided power spectral density $N_0/2$ watts/Hz. Since the subcarriers $a_i(t)$ are statistically independent, $R_{ij}(t, u) = 0$, $i \neq j$, in (1-6). Also since $n(t)$ is a scalar white process, (1-7) becomes

$$K_n(t, u) = \frac{1}{2} N_0 \delta(t-u) . \quad (1-20)$$

then from (1-18)

$$\underline{Q}_n(t, u) = Q_n(t, u) = \frac{2}{N_0} \delta(t-u) , \quad (1-21)$$

and using (1-19) and (1-21), (1-16) and (1-17) reduce to the simple forms

$$\underline{r}_g(t) = \frac{2}{N_0} r(t) , \tag{1-22}$$

and

$$g(t) = \frac{2}{N_0} s(t, \underline{a}(t)) . \tag{1-23}$$

With $s(t, \underline{a}(t))$ a scalar function of the vector $\underline{a}(t)$,

$$\underline{D}(z, \underline{a}(z)) = \begin{bmatrix} \frac{\partial s(z, \underline{a}(z))}{\partial a_1(z)} \\ \cdot \\ \cdot \\ \cdot \\ \frac{\partial s(z, \underline{a}(z))}{\partial a_N(z)} \end{bmatrix} \tag{1-24}$$

From (1-19),

$$\frac{\partial s(z, \underline{a}(z))}{\partial a_j(z)} = \beta_c \sqrt{2P} \cos \left[\omega_c z + \beta_c \sum_{i=1}^N a_i(z) \right] . \tag{1-25}$$

This result is the same for each $j=1, \dots, N$. Substituting (1-22) through (1-25) into (1-15) the j^{th} component of $\hat{\underline{a}}(t)$ is

$$\hat{a}_j(t) = \frac{2}{N_0} \int_{T_i}^{T_f} K_j(t, z) \frac{\partial s(z, \hat{\underline{a}}(z))}{\partial \hat{a}_j(z)} [r(z) - s(z, \hat{\underline{a}}(z))] dz ,$$

where $j=1, \dots, N$ and $T_i \leq t \leq T_f$. (1-26)

The N equations (1-26) can be realized by the feedback system in Fig.13. The operation in (1-26) is the convolution of $K_j(t,z)$ with the "signal"

$$\frac{2}{N_0} \beta_c \sqrt{2P} \cos \hat{\theta}(z) \{r(z) - \sqrt{2P} \sin \hat{\theta}(z)\} \quad (1-27)$$

where

$$\hat{\theta}(t) = \omega_c z + \beta_c \sum_{i=1}^N \hat{a}_i(z) = \omega_c z + \hat{x}(z), \quad T_i \leq z \leq T_f .$$

Since $r(z) = \sqrt{2P} \sin \theta(z) + n(z)$, (1-27) is also equal to

$$\frac{2\beta_c P}{N_0} \left[\sin(\theta(z) + \hat{\theta}(z)) + \sin(\theta(z) - \hat{\theta}(z)) - \sin(2\hat{\theta}(z)) \right. \\ \left. + \sqrt{2/P} n(z) \cos \hat{\theta}(z) \right] \quad (1-28)$$

The noise $n(t)$ is defined to be white with a two-sided spectral density $N_0/2$. This assumption is possible since the spectrum of $n(t)$ is uniform over a broad band around ω_c in the channel carrying $r(t)$. The true spectrum of $n(t)$ is not infinite in width, but this idealization is useful since the correlation function of $n(t)$ is then singular. The spectrum of $n(t)$ is $S_n(\omega)$ depicted in Fig.14. By physical reasoning, $0 \leq W \leq \omega_c$. When $S_n(\omega_c + \Delta) = S_n(\omega_c - \Delta)$ for $0 \leq \Delta \leq W$, there exists the representation

of $n(t)$ given by

$$n(t) = \sqrt{2}[n_1(t) \cos \omega_c t - n_2(t) \sin \omega_c t] , \quad (1-29)$$

where

$$R_n(\tau) = 2R_1(\tau) \cos \omega_c \tau ,$$

and

$$R_1(\tau) = E[n_1(t) n_1(t+\tau)] = E[n_2(t) n_2(t+\tau)] = R_2(\tau) .$$

Since $n(t)$ is Gaussian with zero mean, $n_1(t)$ and $n_2(t)$ are statistically independent Gaussian processes with zero means.

The Fourier transform of $R_n(\tau)$ is

$$S_n(\omega) = S_1(\omega + \omega_c) + S_1(\omega - \omega_c) \quad (1-30)$$

where $S_1(\omega) = F[R_1(\tau)]$. Then

$$S_1(\omega) = S_2(\omega) = \begin{cases} N_0/2 , & |\omega| \leq W \\ 0 , & |\omega| > W \end{cases} \quad (1-31)$$

The spectra $S_1(\omega)$ and $S_2(\omega)$ are also shown in Fig.14. From (1-29),

$$n(z) \cos \hat{\theta}(z) = \frac{1}{\sqrt{2}} \left\{ n_1(z) \cos(2\omega_c z + \hat{x}(z)) - n_2(z) \sin(2\omega_c z + \hat{x}(z)) \right. \\ \left. + n_1(z) \cos \hat{x}(z) + n_2(z) \sin \hat{x}(z) \right\} . \quad (1-32)$$

The spectra of the sine or cosine of $x(t)$ and $\hat{x}(t)$ are lowpass and narrow compared with ω_c and W as indicated in Fig.14. The product of $K_j(t,z)$ and any term of (1-28) at $2\omega_c$ will contribute insignificantly to the value of the integral in (1-26). The part of (1-28) that effects the value of the convolution integral is

$$X_{\text{eff}}(z) = \frac{2P}{N_0} \beta_c \left\{ \sin[x(z) - \hat{x}(z)] \right. \quad (1-33)$$

$$\left. + \frac{1}{\sqrt{P}} [n_1(z) \cos \hat{x}(z) + n_2(z) \sin \hat{x}(z)] \right\}.$$

With the narrowband assumption that gives (1-33), the feedback connection $s(t, \hat{a}(t))$ in Fig.13 can be omitted. Also the term $n_1(z) \cos \hat{x}(z) + n_2(z) \sin \hat{x}(z)$ is white Gaussian noise with a two-sided density spectrum $N_0/2$ (ref.6, section 2.7). The system in Fig.1 follows directly from Fig.13 in light of (1-33).

APPENDIX II

Derivation Of The Lower Bound On
Mean Square Error in Estimating $\underline{a}(t)$

In section 2.3 a realizable approximation of the MAP interval estimator of $\underline{a}(t)$ was given in Fig.2. For large SNR into this realizable demodulator the system became linear, and it was a simple matter to find the system components that gave a MMSE point estimate of $\underline{a}(t)$ at time t . It was also stated in section 2.3 that if sufficient delay was allowed in the post-loop filters $h_{ui}(t)$, $i=1, \dots, N$; the MMSE achieved with the structure of Fig.2 when the input SNR became large was the smallest possible of any point estimator of $\underline{a}(t)$. From 23 the MMSE in the point estimate of the i^{th} component of $\underline{a}(t)$ at t was

$$\sigma_{oi}^2 = \frac{1}{2\pi} \int_{-\infty}^{+\infty} \frac{S_i(\omega) \left[\sum_{j=1, j \neq i}^N S_j(\omega) + N'' \right]}{\sum_{j=1}^N S_j(\omega) + N''} d\omega . \quad (2-1)$$

It is possible to derive a lower bound on the MMSE in point estimating $\underline{a}(t)$ at t that can be achieved with any demodulator, realizable or not. When this bound is computed presently for the MMSE in estimating each component $a_i(t)$ of $\underline{a}(t)$, the bound will be equal to (2-1), $i=1, \dots, N$. This proves that if sufficient

time delay is introduced in the filters $h_{ui}(t)$, the linear demodulator in Fig.4 is the optimum point estimator of $\underline{a}(t)$ at time t in the MMSE sense when the available input is $x(\tau)+n(\tau)$, $-\infty < \tau \leq t$. To invoke Fig.4, however, the input SNR must be large enough that σ_0^2 in (22) is small. For small σ_0^2 , $\sin[x-\tilde{x}] \approx x-\tilde{x}$ in Fig.2, and Fig.4 results. A frequently used threshold of linearity is the value $\sigma_0^2=1/4$. For $\sigma_0^2 < 1/4$, Fig.4 is assumed to apply. Since the mean square error in estimating $x(t)$ by $\tilde{x}(t)$ is σ_0^2 , the Chebychev inequality from probability theory states that (ref.7, page 150)

$$\text{Prob}\{|x(t) - \tilde{x}(t)| > \epsilon\} < \sigma_0^2/\epsilon^2 \quad (2-2)$$

Then the probability that $|x(t) - \tilde{x}(t)|$ exceeds $\pi/4$ radians at time t is less than π^{-2} when $\sigma_0^2 < 1/4$.

The desired lower bound for the mean square error in point estimating $\underline{a}(t)$ at t can be found by first deriving a lower bound for the mean square error interval estimate of $\underline{a}(t)$ on an interval $[T_i, T_f]$, $T_i < T_f$. The mean square error of the interval estimate is defined by (ref.4, section 5.4.4)

$$\underline{R}_I = \frac{1}{[T_f - T_i]} E \left[\int_{T_i}^{T_f} \underline{a}_e(t) \underline{a}_e^T(t) dt \right], \quad (2-3)$$

where $E\{ \}$ is the expected value of the vector random variable generated by the integral operation, and $\underline{a}_e(t)$ is the error

vector defined by (1). A lower bound matrix \underline{R}_B will be found for \underline{R}_I in the sense that $\underline{R}_I - \underline{R}_B$ is nonnegative definite. Referring to (2-3) it is seen that the diagonal terms in the matrix \underline{R}_B represent lower bounds on the mean square errors in estimating $a_i(t)$, $i=1, \dots, N$.

The lower bound matrix \underline{R}_B is defined by

$$\underline{R}_B = \frac{1}{[T_f - T_i]} \int_{T_i}^{T_f} \underline{J}^{-1}(t', t') dt' \tag{2-4}$$

where $\underline{J}^{-1}(t', x)$ is the inverse of the information matrix kernel $\underline{J}(t', x)$ and is defined by the matrix integral equation (ref.4, page 454)

$$\begin{aligned} \underline{J}^{-1}(t', x) + \int_{T_i}^{T_f} \int_{T_i}^{T_f} \underline{J}^{-1}(t', u) \cdot \\ \left\{ E \left[\underline{D}(u, \underline{a}(u)) \underline{Q}_n(u, z) \underline{D}^T(z, \underline{a}(z)) \right] \right\} \underline{K}_a(z, x) du dz \\ = \underline{K}_a(t', x), \quad \text{where} \quad T_i \leq t', \quad x \leq T_f \quad . \end{aligned} \tag{2-5}$$

To find lower bounds on the elements of \underline{R}_I , (2-5) must be solved and (2-4) must be evaluated with $x=t'$. For the scalar signal $s(t, \underline{a}(t)) = \sqrt{2P} \sin \left[\omega_c t + \beta_c \sum_{i=1}^N a_i(t) \right]$ that is a function of the vector $\underline{a}(t)$, and the scalar additive noise $n(t)$ with uniform

spectral density $N_0/2$; the inverse kernel vector

$\underline{Q}_n(u, z) = (2/N_0) \delta(u-z)$, an impulse of weight $2/N_0$ at $z=u$, and $\underline{D}(u, \underline{a}(u))$ is the vector,

$$\underline{D}(u, \underline{a}(u)) = \begin{bmatrix} \frac{\partial s(u, \underline{a}(u))}{\partial a_1(u)} \\ \cdot \\ \cdot \\ \cdot \\ \frac{\partial s(u, \underline{a}(u))}{\partial a_N(u)} \end{bmatrix} \quad (2-6)$$

If

$$d_{si}(u, \underline{a}(u)) = \frac{\partial s(u, \underline{a}(u))}{\partial a_i(u)}$$

and

$$E\left\{d_{si}(u, \underline{a}(u)) \quad d_{sj}(z, \underline{a}(z))\right\} = R_{ds}^{ij}(u, z) \quad (2-7)$$

then

$$E\left\{\underline{D}(u, \underline{a}(u)) \quad \underline{D}^T(z, \underline{a}(z))\right\} = \underline{R}_{ds}(u, z) \quad (2-8)$$

where the term in the i^{th} row and j^{th} column of the $N \times N$ matrix \underline{R}_{ds} is just $R_{ds}^{ij}(u, z)$. Substituting the $2/N_0$ valued impulse for $\underline{Q}_n(u, z)$ and (2-8) into (2-5) gives

$$\underline{J}^{-1}(t', x) + \frac{2}{N_0} \int_{T_i}^{T_f} \underline{J}^{-1}(t', u) \underline{R}_{ds}(u, u) \underline{K}_a(u, x) du = \underline{K}_a(t', x) \quad ,$$

for $T_i \leq t', x \leq T_f$. (2-9)

that is an $N \times N$ matrix with all off diagonal terms equal to zero.

The matrix $\underline{J}^{-1}(t', x)$ is

$$\underline{J}^{-1} = \begin{bmatrix} J_{11}^{-1} & \cdot & \cdot & \cdot & J_{1N}^{-1} \\ \cdot & \cdot & \cdot & \cdot & \cdot \\ \cdot & \cdot & J_{ij}^{-1} & \cdot & \cdot \\ \cdot & \cdot & \cdot & \cdot & \cdot \\ J_{N1}^{-1} & \cdot & \cdot & \cdot & J_{NN}^{-1} \end{bmatrix} \quad (2-12)$$

Post multiplication of (2-12) by the unit vector \underline{I} gives

$$\underline{J}^{-1} \underline{I} = \begin{bmatrix} \sum_{j=1}^N J_{1j}^{-1} \\ \cdot \\ \cdot \\ \sum_{j=1}^N J_{ij}^{-1} \\ \cdot \\ \cdot \\ \sum_{j=1}^N J_{Nj}^{-1} \end{bmatrix} \quad (2-13)$$

Premultiplication of (2-11) by \underline{I}^T gives

$$\underline{I}^T \underline{K}_a = [K_1 \cdot \cdot \cdot K_i \cdot \cdot \cdot K_N] \cdot \quad (2-14)$$

Then the integrand of (2-9) is

$$P \beta_C^2 \underline{J}^{-1}(t', u) \underline{I} \underline{I}^T \underline{K}_a(u, x) = \tag{2-15}$$

$$P \beta_C^2 \begin{bmatrix} K_1(u, x) \sum_{j=1}^N J_{1j}^{-1}(t', u) \cdots K_N(u, x) \sum_{j=1}^N J_{1j}^{-1}(t', u) \\ \cdot \\ \cdot \\ \cdot \\ K_i(u, x) \sum_{j=1}^N J_{ij}^{-1}(t', u) \\ \cdot \\ \cdot \\ K_1(u, x) \sum_{j=1}^N J_{Nj}^{-1}(t', u) \cdots K_N(u, x) \sum_{j=1}^N J_{Nj}^{-1}(t', u) \end{bmatrix} \cdot$$

The term in the r th row and p th column of \underline{K}_a can be denoted as K_{rp} and when $r=p=i$, $K_{rp}=K_i$. From (2-11) $K_{rp}=0$ if $r \neq p$. From (2-9) the term $K_{rp}(t', x)$ is given by the scalar integral equation

$$J_{rp}^{-1}(t', x) + \frac{1}{N^w} \int_{T_i}^{T_f} K_p(u, x) \sum_{j=1}^N J_{rj}^{-1}(t', u) du = \begin{cases} K_r(t', x), & r=p \\ 0 & , r \neq p \end{cases}$$

for $1 \leq r, p \leq N$. and $T_i \leq t', x \leq T_f$. (2-16)

The set of N^2 equations described by (2-16) can be solved simultaneously for $J_{rp}^{-1}(t', x)$. For fixed r , consider the sum of (2-16) over all p . This is

$$\sum_{p=1}^N J_{rp}^{-1}(t', x) + \frac{1}{N''} \int_{T_i}^{T_f} \left[\sum_{p=1}^N K_p(u, x) \right] \left[\sum_{j=1}^N J_{rj}^{-1}(t', u) \right] du = K_r(t', x) ,$$

$$\text{for } 1 \leq r \leq N ; T_i \leq t', x \leq T_f . \quad (2-17)$$

But with $h_r(t', x) = \sum_{p=1}^N J_{rp}^{-1}(t', x)$, (2-17) has the form of the

Wiener-Hopf integral equation

$$\frac{1}{N''} \int_{T_i}^{T_f} \left[N'' \delta(u-x) + \sum_{p=1}^N K_p(u, x) \right] h_r(t', u) du = K_r(t', x) , \quad (2-18)$$

$$\text{for } 1 \leq r \leq N , T_i \leq t', x \leq T_f .$$

If $h_r(t', x)$ is found by solving (2-18), this can be used to find $J_{rp}^{-1}(t', x)$, $p \neq r$, directly from (2-16). In this manner all $J_{rp}^{-1}(t', x)$ are found for $1 \leq r, p \leq N$.

The solution of (2-18) is difficult for most cases. One class of problems where the solution of (2-18) is direct is where $a(t)$ is stationary and $T_i \rightarrow -\infty$ (ref.4, page 444). Then $K_r(t', x) \rightarrow K_r(t'-x)$ and $h_r(t', u) \rightarrow h_r(t'-u)$. If in addition $T_f \rightarrow +\infty$,

the solution of (2-18) is simple, as can be seen by considering

$$\frac{1}{N''} \int_{-\infty}^{+\infty} \left[N'' \delta(u-x) + \sum_{p=1}^N K_p(u-x) \right] h_r(t'-u) du = K_r(t'-x) ,$$

$$\text{for } 1 \leq r \leq N \quad \text{and} \quad -\infty < t' , x < +\infty . \quad (2-19)$$

With the change of variables $t'-x=\tau$ and $v=t'-u$, $u-x=\tau-v$, $u=-\infty \rightarrow v=+\infty$, $u=+\infty \rightarrow v=-\infty$, and $dv=-du$. Then (2-19) becomes

$$\frac{1}{N''} \int_{-\infty}^{+\infty} \left[N'' \delta(\tau-v) + \sum_{p=1}^N K_p(\tau-v) \right] h_r(v) dv = K_r(\tau) , \quad (2-20)$$

$$\text{for} \quad -\infty < \tau < +\infty .$$

Since (2-20) is defined for $-\infty < \tau < +\infty$, the Fourier transform of each side can be taken, and since the left side is a convolution integral, the result is

$$H_r(j\omega) = N'' S_r(\omega) / \left[N'' + \sum_{p=1}^N S_p(\omega) \right] , \quad -\infty < \omega < +\infty . \quad (2-21)$$

where $H_r(j\omega) = F[h_r(v)]$ and $S_r(\omega) = F[K_r(\tau)]$ for $1 \leq r \leq N$.

For the stationary problem with $T_i \rightarrow -\infty$, $T_f \rightarrow +\infty$, $t'-x=\tau$ and $v=t'-u$, (2-16) becomes

$$J_{rp}^{-1}(\tau) = -\frac{1}{N''} \int_{-\infty}^{+\infty} K_p(\tau-v) h_r(v) dv, \quad (2-22)$$

for $p \neq r$ and $-\infty < \tau < +\infty$.

This can be transformed to give

$$F \left[J_{rp}^{-1}(\tau) \right] = -\frac{S_p(\omega) S_r(\omega)}{N'' + \sum_{p=1}^N S_p(\omega)}, \quad r \neq p. \quad (2-23)$$

Since

$$H_r(j\omega) = \sum_{j=1}^N F \left[J_{rj}^{-1}(\tau) \right]$$

the transform of $J_{rr}^{-1}(\tau)$ follows by subtracting all $F \left[J_{rp}^{-1}(\tau) \right]$, $r \neq p$,

from $H_r(j\omega)$. Then for $1 \leq r \leq N$,

$$F \left[J_{rr}^{-1}(\tau) \right] = \frac{S_r(\omega) \left[N'' + \sum_{p=1, p \neq r}^N S_p(\omega) \right]}{N'' + \sum_{p=1}^N S_p(\omega)}, \quad (2-24)$$

The value $J_{rr}^{-1}(0)$ is a lower bound on the error in estimating $a_r(t)$ on the interval $(-\infty, \infty)$ given $x(\tau) + n''(\tau)$ for $-\infty < \tau < +\infty$.

If only $x(\tau) + n''(\tau)$, $-\infty < \tau \leq t$ is given, but the estimate is delayed in time by δ , $J_{rr}^{-1}(0)$ is again the lower bound on estimating $a_r(t)$ on the interval $(-\infty, t]$ as $\delta \rightarrow +\infty$. Since

$$J_{rr}^{-1}(0) = \frac{1}{2\pi} \int_{-\infty}^{\infty} F \left[J_{rr}^{-1}(\tau) \right] d\omega, \quad (2-25)$$

substitution of (2-24) gives

$$\sigma_r^2(I) \geq \frac{1}{2\pi} \int_{-\infty}^{+\infty} \frac{S_r(\omega) [S_x(\omega) - S_r(\omega) + N'']}{[S_x(\omega) + N'']} d\omega \quad (2-26)$$

where $\sigma_r^2(I)$ is the mean square error in the interval estimate of $a_r(t)$ on $(-\infty, t]$ with delay $\delta \rightarrow +\infty$. Since $J_{rr}^{-1}(0)$ is the same for each t , it is also equal to the lower bound on the mean square error in point estimating $a_r(t)$ at t given $x(\tau) + n''(\tau)$, $-\infty < \tau \leq t$, and delay $\delta \rightarrow +\infty$. But the MMSE for the point estimation of $a_r(t)$ using the system in Fig.4 was derived in section 2-6 as σ_{0r}^2 in (23). Since $J_{rr}^{-1}(0)$ and σ_{0r}^2 are the same, the system in Fig.4 is the optimum point estimator of $a(t)$ at t in the MMSE sense when delay $\delta \rightarrow +\infty$ is allowed for $h_{ui}(t)$, $i=1, \dots, N$.

APPENDIX III

Derivation Of The Transfer Function $H_i(j\omega)$ In Equation (18)

To compute the optimum linear filters $h_{ui}(t)$ in Fig.4, it is necessary to derive the transfer function from the input of Fig.4 to the point of the response $\tilde{a}_{ri}(t)$. By definition this transfer function is

$$H_i(j\omega) = \tilde{A}_{ri}(j\omega) / X(j\omega) ; \quad i=1, \dots, N. \quad (3-1)$$

From Fig.4 the Fourier transform of $\tilde{a}_{ri}(t)$ is

$$\tilde{A}_{ri}(j\omega) = H_{ri}(j\omega) [X(j\omega) - Y(j\omega)] ; \quad i=1, \dots, N ; \quad (3-2)$$

where

$$K = 1/N'' = 2P \beta_c^2 / N_o \quad \text{and} \quad Y(j\omega) = \sum_{i=1}^N A_{ri}(j\omega) .$$

Combining (3-1) and (3-2) gives

$$H_i(j\omega) = \frac{KH_{ri}(j\omega)}{1 + KH_{ri}(j\omega)} \left[1 - \sum_{k=1, k \neq i}^N H_k(j\omega) \right] , \quad (3-3)$$

for $i=1, \dots, N$.

There are N independent equations in the N transfer functions $H_i(j\omega)$. This system could be solved directly, but it is simpler to find the $H_i(j\omega)$ by the following argument.

The transform $\tilde{A}_{r1}(j\omega)$ is the response of the feedback system in Fig.15. If (J), $J=1, \dots, N$ denotes the input of the J^{th} summing point from the left in Fig.15, and (0) is the output point of the amplifier K; the transfer function from (J) to (0) is a member of the sequence,

$$\begin{aligned}
 \text{(N) to (0):} \quad G_N &= K/[1 + K H_{rN}] , & (3-4) \\
 \text{(N-1) to (0):} \quad G_{N-1} &= G_N/[1 + G_N H_{r(N-1)}] , \\
 &\vdots \\
 \text{(J) to (0):} \quad G_J &= G_{J+1}/[1 + G_{J+1} H_{rJ}] , \\
 &\vdots \\
 \text{(2) to (0)} \quad G_2 &= G_3/[1 + G_3 H_{r2}] ,
 \end{aligned}$$

The transfer function from (1) to $\tilde{A}_{r1}(j\omega)$ is

$$H_1(j\omega) = G_2(j\omega) H_{r1}(j\omega)/[1 + G_2(j\omega) H_{r1}(j\omega)] \quad (3-5)$$

Substitution of G_N into G_{N-1} , G_{N-1} into G_{N-2} , etc.

gives

$$H_1(j\omega) = K H_{r1}(j\omega) / \left[1 + K \sum_{i=1}^N H_{ri}(j\omega) \right] \quad (3-6)$$

This is (19) for $i=1$. By symmetry,

$$H_i(j\omega) = K H_{ri}(j\omega) / \left[1 + K \sum_{i=1}^N H_{ri}(j\omega) \right], \quad (3-7)$$

for $i=1, \dots, N$.

Substitution of (3-7) into (3-3) leads to an identity. That is, (3-7) checks as the solution of (3-3)

APPENDIX IV

An Example Where $N=2$ And $S_1(\omega) S_2(\omega) \neq 0$

Let
$$S_x(\omega) = S_1(\omega) + S_2(\omega)$$

where

$$S_1(\omega) = 2a_1 p_1 / (\omega^2 + p_1^2)$$

and

$$S_2(\omega) = a_2 p_2 / [(\omega + \omega_2)^2 + p_2^2] + a_2 p_2 / [(\omega - \omega_2)^2 + p_2^2] \quad (4-1)$$

Then

$$1 + \frac{S_x(\omega)}{N''} = \frac{A(1) s^6 + A(2) s^4 + A(3) s^2 + A(4)}{[\omega^2 + p_1^2][(\omega + \omega_2)^2 + p_2^2][(\omega - \omega_2)^2 + p_2^2]} \quad (4-2)$$

where $s=j\omega$ and the A's are as follows,

$$A(1) = -1$$

$$A(2) = \{ [p_1^2 - 2(\omega_2^2 - p_2^2)] + 2(a_1 p_1 + a_2 p_2) / N'' \}$$

$$A(3) = -\{ [(\omega_2^2 + p_2^2)^2 - 2p_1^2(\omega_2^2 - p_2^2)] - 4a_1 p_1(\omega_2^2 - p_2^2) / N'' + 2a_2 p_2(\omega_2^2 + p_2^2 + p_1^2) / N'' \}$$

$$A(4) = \{ p_1^2(\omega_2^2 + p_2^2)^2 + 2a_1 p_1(\omega_2^2 + p_2^2)^2 / N'' + 2a_2 p_2 p_1^2(\omega_2^2 + p_2^2) / N'' \}$$

The parameters to be selected are $p_1, p_2, a_1, a_2, \omega_2$ and N'' .

Since $S_x(\omega)$ is a function of ω^2 , we can write

$$1 + S_x(\omega)/N'' = \Psi(\omega) \Psi^*(\omega) = \prod_{k=1}^3 \frac{\omega^2 + \beta_k^2}{\omega^2 + \gamma_k^2}$$

where β_k and γ_k have positive real parts and $\Psi(\omega) =$

$$\prod_{k=1}^3 (\omega - j\beta_k) / (\omega - j\gamma_k)$$

consists of all factors of $1 + S_x(\omega)/N''$ in

the upper half of the ω -plane. The factor $\Psi^*(\omega)$ is the conjugate of $\Psi(\omega)$. Then $\Psi(\omega) = [1 + S_x(\omega)/N'']^+$ and $\Psi^*(\omega) = [1 + S_x(\omega)/N'']^-$.

The transfer function of the optimum realizable filter for estimating $x(t)$ from $x(\tau) + n''(\tau)$, $\tau \leq t$, is from (14)

$$H_{ol}(j\omega) = 1 - \frac{1}{\Psi(\omega)} .$$

Then (15) gives

$$H_{r1}(j\omega) + H_{r2}(j\omega) = K^{-1} (\Psi(\omega) - 1)$$

$$= K^{-1} \frac{\left[\prod_{k=1}^3 (\omega - j\beta_k) - \prod_{k=1}^3 (\omega - j\gamma_k) \right]}{\prod_{k=1}^3 (\omega - j\gamma_k)} \quad (4-3)$$

The poles $j\gamma_k$ of $\Psi(\omega)$ follow directly from the quadratic factors in the denominator of $1+S_x(\omega)/N^n$. These are

$$j\gamma_1 = jp_1, \quad j\gamma_2 = jp_2 - \omega_2 \quad \text{and} \quad j\gamma_3 = jp_2 + \omega_2$$

The zeros $j\beta_k$ of $\Psi(\omega)$ must be found by factoring the sixth order polynomial in the numerator of $1+S_x(\omega)/N^n$.

The poles of $H_{r1}+H_{r2}$ are simple. The function H_{r1} is associated with the pole $j\gamma_1$ and H_{r2} with the remainder, since $j\gamma_1$ is the only pole arising from $S_1(\omega)$. Using a partial fraction expansion for $H_{r1}+H_{r2}$ as in (16) gives

$$H_{r1}(j\omega) = k_1/(\omega-j\gamma_1)$$

and

$$H_{r2}(j\omega) = k_2/(\omega-j\gamma_2) + k_3/(\omega-j\gamma_3) ,$$

where

$$k_1 = \frac{-jN^n \prod_{k=1}^3 (\beta_k - p_1)}{(p_1 - p_2)^2 + \omega_2^2}$$

$$k_2 = \frac{-jN^n \prod_{k=1}^3 (\beta_k - p_2 - j\omega_2)}{(p_1 - p_2 - j\omega_2)(-j2\omega_2)} = -jN^n A$$

$$k_3 = \frac{-jN^n \prod_{k=1}^3 (\beta_k - p_2 + j\omega_2)}{(p_1 - p_2 + j\omega_2)(j2\omega_2)} = -jN^n A^*$$

The conjugate relationship between jk_2 and jk_3 follows from the property

$$\prod_{k=1}^3 (\beta_k - \gamma_2) = \prod_{k=1}^3 (\beta_k^* - \gamma_2) = \prod_{k=1}^3 (\beta_k - \gamma_3)^* .$$

Then

$$H_{r1}(j\omega) = N'' \prod_{k=1}^3 (\beta_k - p_1) / [(p_1 - p_2)^2 + \omega_2^2] (j\omega + p_1) \quad (4-4)$$

and

$$H_{r2}(j\omega) = N'' \left[\frac{A}{(j\omega + \gamma_2)} + \frac{A^*}{(j\omega + \gamma_2^*)} \right]$$

where

$$A = \prod_{k=1}^3 (\beta_k - p_2 - j\omega_2) / (p_1 - p_2 - j\omega_2) (-2j\omega_2) .$$

The two terms of H_{r2} combine to give

$$H_{r2}(j\omega) = N'' \left[\frac{(j\omega)^2 \operatorname{Re}[A] + 2 \operatorname{Re}[A(p_2 - j\omega_2)]}{(j\omega)^2 + 2p_2(j\omega) + p_2^2 + \omega_2^2} \right] \quad (4-5)$$

where $\operatorname{Re}[\]$ denotes the real part.

The minimum mean-square error in estimating $x(t)$ given $x(\tau)+n''(\tau)$, $\tau \leq t$, is known from (22) as a function of β_k , γ_k , and N'' . This error is also given by (ref.6, page 146)

$$\sigma_o^2 = N'' \sum_{k=1}^3 (\beta_k - \gamma_k) = N'' \left[\sum_{k=1}^3 \beta_k - (p_1 + 2p_2) \right] \quad (4-6)$$

The optimum realizable filters with δ -sec delay for estimating $a_1(t)$ and $a_2(t)$ given the input $x(\tau)+n''(\tau)$, $\tau \leq t$, have been derived. For $i=1$ and 2

$$H_{oi}^u(j\omega) = H_{oi}^u(j\omega) \exp[-j\omega\delta]$$

where from (17)
$$H_{oi}^u(j\omega) = \frac{S_i(\omega)}{N''\Psi(\omega)\Psi^*(\omega)}$$

Then

$$H_{o1}^u(j\omega) = \frac{1}{N''} \cdot \frac{2a_1 p_1 [\omega^4 + 2(p_2^2 - \omega_2^2)\omega^2 + (\omega_2^2 + p_2^2)^2]}{P(\omega)}, \quad (4-7)$$

and

$$H_{o2}^u(j\omega) = \frac{1}{N''} \cdot \frac{2a_2 p_2 [\omega^4 + (\omega_2^2 + p_2^2 + p_1^2)\omega^2 + (\omega_2^2 + p_2^2)p_1^2]}{P(\omega)} \quad (4-8)$$

where
$$P(\omega) = -A(1)\omega^6 + A(2)\omega^4 - A(3)\omega^2 + A(4).$$

From (23) the lower bounds on the mean-square errors in estimating $a_1(t)$ and $a_2(t)$ with delay are, respectively,

$$\sigma_{o1}^2 = \int_{-\infty}^{+\infty} \frac{S_1(\omega) [S_2(\omega) + S_{n''}(\omega)]}{S_1(\omega) + S_2(\omega) + S_{n''}(\omega)} \frac{d\omega}{2\pi} \quad (4-9)$$

and

$$\sigma_{o2}^2 = \int_{-\infty}^{+\infty} \frac{S_2(\omega) [S_1(\omega) + S_{n''}(\omega)]}{S_1(\omega) + S_2(\omega) + S_{n''}(\omega)} \frac{d\omega}{2\pi} \quad (4-10)$$

These errors are obtained in the limit as $\delta \rightarrow \infty$. For sufficiently large delay, these are the mean-square errors for optimum estimation of $a_1(t)$ and $a_2(t)$ at time $t+\delta$ given the input $x(\tau)+n''(\tau)$ for $\tau \leq t$.

Since

$$H_{oi}^u(j\omega) = S_i(\omega)/N'' \Psi(\omega) \Psi^*(\omega)$$

and $\Psi(\omega) \Psi^*(\omega) = 1 + S_x(\omega)/N''$,

$$\sigma_{oi}^2 = \int_{-\infty}^{+\infty} \frac{S_1(\omega) S_2(\omega)}{N'' \Psi(\omega) \Psi^*(\omega)} \frac{d\omega}{2\pi} + \int_{-\infty}^{+\infty} N'' H_{oi}^u(j\omega) \frac{d\omega}{2\pi}$$

where $S_1(\omega) S_2(\omega)/N'' \Psi(\omega) \Psi^*(\omega) =$

$$\frac{4a_1 a_2 p_1 p_2 [\omega^4 + (\omega_2^2 + p_2^2 + p_1^2) \omega^2 + p_1^2 (\omega_2^2 + p_2^2)]}{N'' P(\omega)}$$

Then

$$\begin{aligned} \sigma_{O1}^2 = & \int_{-\infty}^{+\infty} \frac{d\omega}{2\pi} \{ (N'' 2a_1 p_1 + 4a_1 p_1 a_2 p_2) \omega^4 + \\ & [N'' 4a_1 p_1 (p_2^2 - \omega_2^2) + 4a_1 p_1 a_2 p_2 (\omega_2^2 + p_2^2 + p_1^2)] \omega^2 + \\ & [N'' 2a_1 p_1 (\omega_2^2 + p_2^2)^2 + 4a_1 p_1 a_2 p_2 p_1^2 (\omega_2^2 + p_2^2)] \} / N'' P(\omega) \end{aligned} \quad (4-11)$$

and

$$\begin{aligned} \sigma_{O2}^2 = & \int_{-\infty}^{+\infty} \frac{d\omega}{2\pi} \{ (N'' 2a_2 p_2 + 4a_1 p_1 a_2 p_2) \omega^4 + \\ & [N'' 2a_2 p_2 + 4a_1 p_1 a_2 p_2] (\omega_2^2 + p_2^2 + p_1^2) \omega^2 + \\ & [N'' 2a_2 p_2 + 4a_1 p_1 a_2 p_2] (\omega_2^2 + p_2^2) p_1^2 \} / N'' P(\omega) \end{aligned} \quad (4-12)$$

If N_1 and N_2 are two values of N'' the assumption

$$\frac{S_1(\omega) [S_2(\omega) + N_1]}{S_1(\omega) + S_2(\omega) + N_1} \geq \frac{S_1(\omega) [S_2(\omega) + N_2]}{S_1(\omega) + S_2(\omega) + N_2}$$

implies $N_1 \geq N_2$. Similarly for the case where the rolls of S_1 and S_2 are interchanged. Hence $N_1 \geq N_2 \rightarrow \sigma_{O1}^2(N_1) \geq \sigma_{O1}^2(N_2)$ and $\sigma_{O2}^2(N_1) \geq \sigma_{O2}^2(N_2)$. The mean square errors are monotonic with N'' .

The error integrals have the simple form

$$\sigma_{O1}^2 = \frac{1}{2\pi N''} \int_{-\infty}^{+\infty} \frac{C(1)\omega^4 + C(2)\omega^2 + C(3)}{P(\omega)} d\omega, \quad (4-13)$$

and

$$\sigma_{O2}^2 = \frac{1}{2\pi N''} \int_{-\infty}^{+\infty} \frac{D(1)\omega^4 + D(2)\omega^2 + D(3)}{P(\omega)} d\omega, \quad (4-14)$$

where $P(\omega) = -A(1)\omega^6 + A(2)\omega^4 - A(3)\omega^2 + A(4) = \prod_{k=1}^3 (\omega^2 + \beta_k^2)$

and the C's and D's are constants. Since $P(\omega)$ is two orders greater than the integrand numerator for each integral, the theory of residues can be used to evaluate σ_{O1}^2 and σ_{O2}^2 . More specifically (ref.8, page 368) if $Q(z)$ is a function analytic in the upper half of the z -plane except at a finite number of poles, none of which lies on the real axis, and if $|zQ(z)|$ converges uniformly to zero as $z \rightarrow \infty$ through values for which $0 \leq \arg z \leq \pi$,

then $\int_{-\infty}^{+\infty} Q(\omega)d\omega$ is equal to $2\pi j$ times the sum of the residues at the poles of $Q(z)$ in the upper half of the z -plane. Letting $Q_1(\omega)$ and $Q_2(\omega)$ be the integrands in σ_{O1}^2 and σ_{O2}^2 , it is not difficult to show that the requirements of the residue theorem hold at least for the values of the A's, C's and D's used. Hence to evaluate σ_{O1}^2 and σ_{O2}^2 the residues of $Q_1(z)$ and $Q_2(z)$, respectively, are evaluated in the upper half of the z -plane.

Since

$$P(z) = \prod_{k=1}^3 (z + j\beta_k)(z - j\beta_k)$$

where $\text{Re}[\beta_k] > 0$ for $k=1,2,3$; the roots of $P(z)$ with positive imaginary parts must be $z = +j\beta_k$, $k=1,2$ and 3 . Then

$$(1) \quad Q_1(z) = \frac{C(1)z^4 + C(2)z^2 + C(3)}{\prod_{k=1}^3 (z + j\beta_k)(z - j\beta_k)}$$

and

$$(2) \quad Q_2(z) = \frac{D(1)z^4 + D(2)z^2 + D(3)}{\prod_{k=1}^3 (z + j\beta_k)(z - j\beta_k)}$$

For (1), the residue at $j\beta_r$, $r=1,2,3$ is defined by

$$\begin{aligned} R_r^{(1)} &= \lim_{z \rightarrow j\beta_r} (z - j\beta_r) Q_1(z) \\ &= \frac{C(1)(j\beta_r)^4 + C(2)(j\beta_r)^2 + C(3)}{\prod_{k=1}^3 (j\beta_r + j\beta_k) \cdot \prod_{\substack{k=1 \\ k \neq r}}^3 (j\beta_r - j\beta_k)}, \quad r=1,2,3 \end{aligned} \quad (4-15)$$

For (2), the residue at $j\beta_r$, $r=1,2,3$ is

$$\begin{aligned} R_r^{(2)} &= \frac{D(1)(j\beta_r)^4 + D(2)(j\beta_r)^2 + D(3)}{\prod_{k=1}^3 (j\beta_r + j\beta_k) \cdot \prod_{\substack{k=1 \\ k \neq r}}^3 (j\beta_r - j\beta_k)}, \quad r=1,2,3 \end{aligned} \quad (4-16)$$

By the residue theorem

$$\sigma_{oq}^2 = \frac{j}{N^n} \sum_{r=1}^3 R_r^{(q)}, \quad q=1,2. \quad (4-17)$$

The transfer function from the demodulator input to the point of the response $\tilde{a}_{ri}(t)$ was found to be

$$H_i(j\omega) = \tilde{A}_{ri}(j\omega)/X(j\omega) = H_{ri}(j\omega)/N^n [1 + S_x(\omega)/N^n]^+ \quad (4-18)$$

Assuming a delay of $\delta > 0$ sufficiently large, the post loop filter h_{ui} has the transfer function $H_{ui}(j\omega) = H_{oi}(j\omega)/H_i(j\omega)$ that is closely approximated by a realizable transfer function. Substituting $H_{o1}(j\omega)$ and $H_1(j\omega)$ gives

$$H_{u1}(j\omega) = \frac{2a_1 p_1 [(p_1 - p_2)^2 + \omega_2^2] [j\omega - p_2 + j\omega_2] [j\omega - p_2 - j\omega_2] \exp[-j\omega\delta]}{N^n \prod_{k=1}^3 (\beta_k - p_1) (j\omega - \beta_1) (j\omega - \beta_2) (j\omega - \beta_3)} \quad (4-19)$$

Substituting $H_{o2}(j\omega)$ and $H_2(j\omega)$ gives

$$H_{u2}(j\omega) = \frac{2a_2 p_2 (j\omega - p_1) (j\omega + \sqrt{\omega_2^2 + p_2^2}) (j\omega - \sqrt{\omega_2^2 + p_2^2}) \exp[-j\omega\delta]}{N^n \{2\text{Re}[A](j\omega) + 2\text{Re}[A(p_2 - j\omega_2)]\} \prod_{k=1}^3 (j\omega - \beta_k)} \quad (4-20)$$

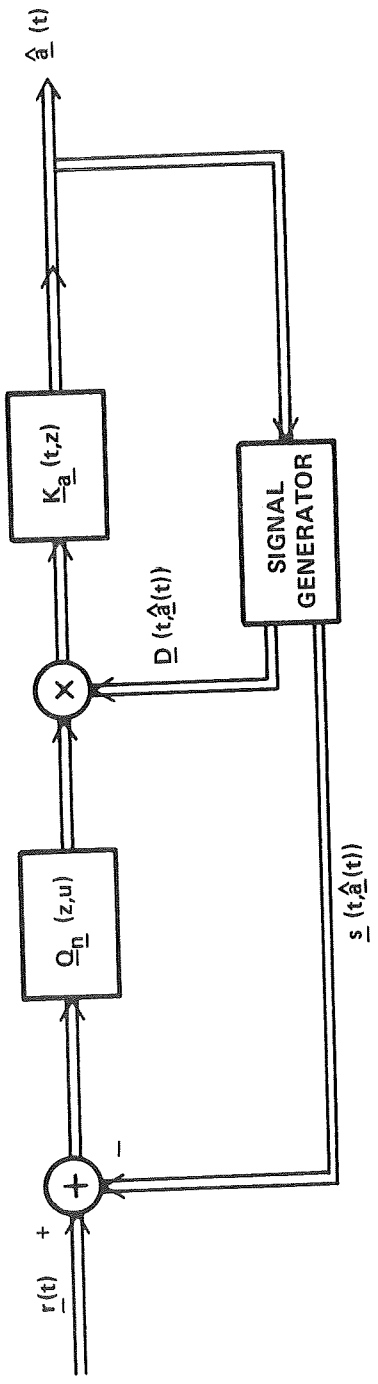


FIGURE 12 - FEEDBACK SYSTEM REPRESENTATION OF THE MAP INTERVAL ESTIMATE EQUATIONS FOR THE NO-MEMORY MODULATION PROBLEM

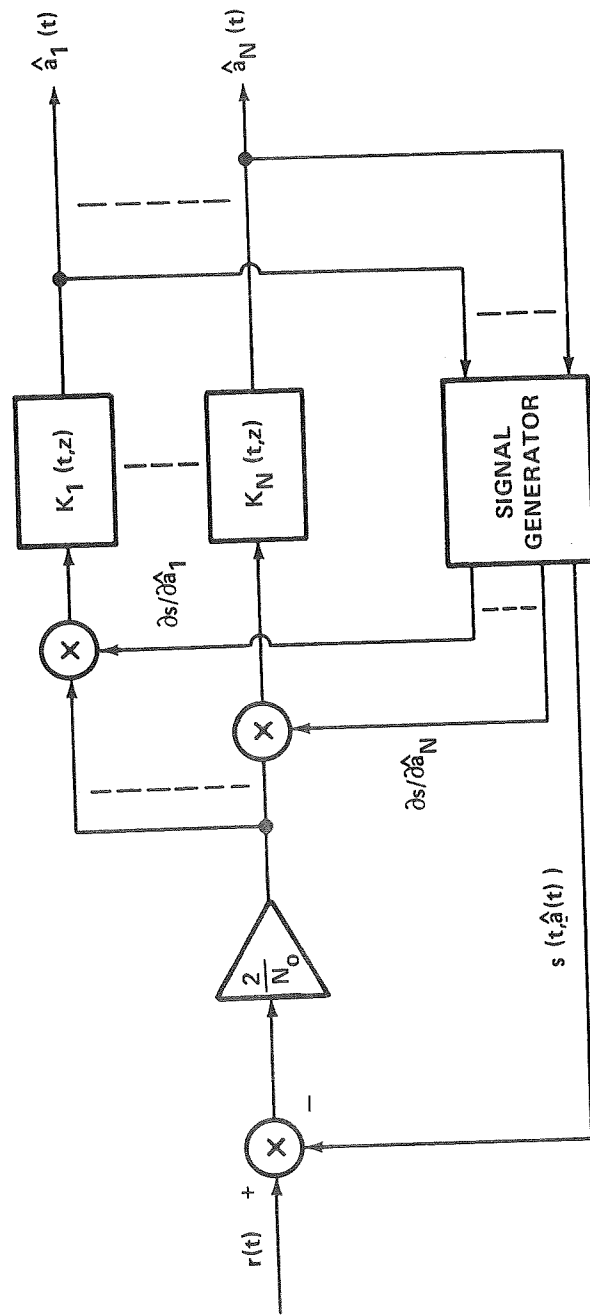


FIGURE 13 - FEEDBACK SYSTEM REPRESENTATION OF (1-26), THE INTERVAL ESTIMATION OF MULTIPLE PHASE MODULATING SUBCARRIERS.

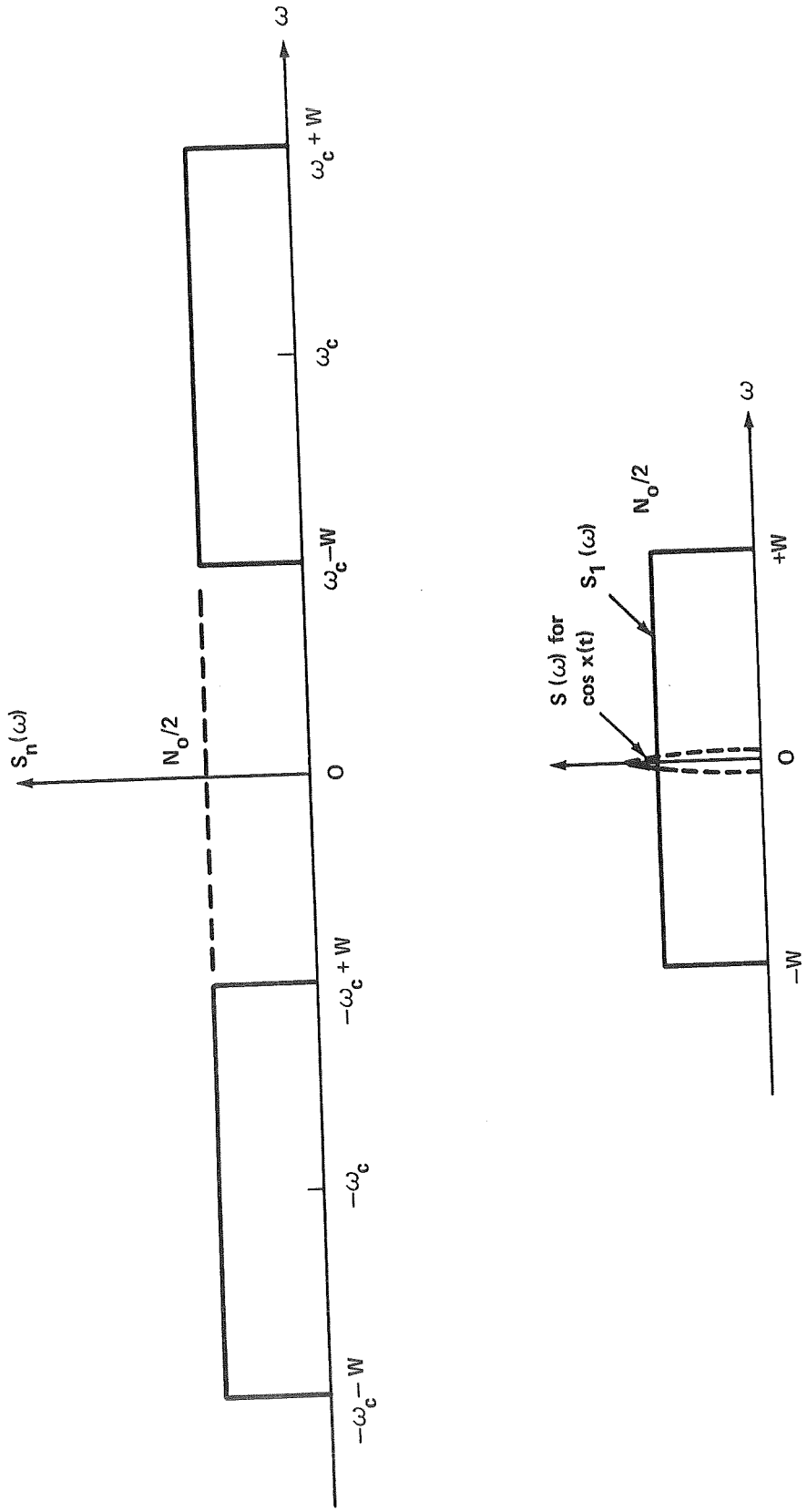


FIGURE 14 - REPRESENTATIVE SPECTRUM OF UNIFORM BANDPASS NOISE $N(t)$ COMPARED WITH THE SPECTRUM OF $\cos x(t)$

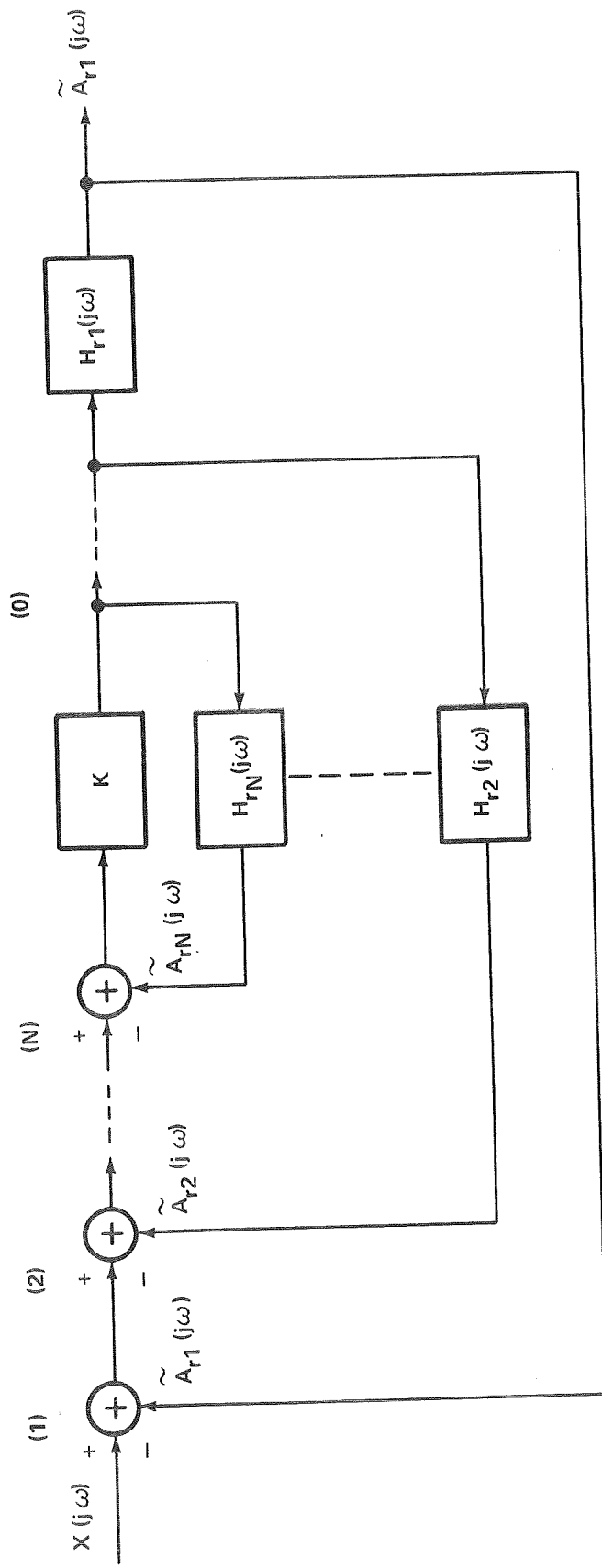


FIGURE 15 - A FEEDBACK SYSTEM USED TO DETERMINE $H_{ri}(j\omega)$ IN TERMS OF $H_{ri}(j\omega)$, $i = 1, \dots, N$.